Title

Insulin-like growth factor-1 activates AMPK to augment mitochondrial function and correct neuronal metabolism in sensory neurons in type 1 diabetes

Authors

Aghanoori, Mohamad-Reza
Smith, Darrell R
Shariati-Ievari, Shiva
et al.

Publication Date

2019-02-01

DOI

10.1016/j.molmet.2018.11.008

Peer reviewed

Original Article

MOLECULAR METABOLISM

Insulin-like growth factor-1 activates AMPK to augment mitochondrial function and correct neuronal metabolism in sensory neurons in type 1 diabetes

Mohamad-Reza Aghanoori [1,2], Darrell R. Smith [1], Shiva Shariati-levari [5], Andrew Ajisebutu [1], Annee Nguyen [3], Fiona Desmond [3], Carlos H.A. Jesus [3], Xiajun Zhou [3], Nigel A. Calcutt [3], Michel Aliani [4,5,6], Paul Fernyhough [1,2,*]

ABSTRACT

Objective: Diabetic sensorimotor polyneuropathy (DSPN) affects approximately half of diabetic patients leading to significant morbidity. There is impaired neurotrophic growth factor signaling, AMP-activated protein kinase (AMPK) activity and mitochondrial function in dorsal root ganglia (DRG) of animal models of type 1 and type 2 diabetes. We hypothesized that sub-optimal insulin-like growth factor 1 (IGF-1) signaling in diabetes drives loss of AMPK activity and mitochondrial function, both contributing to development of DSPN.

Methods: Age-matched control Sprague-Dawley rats and streptozotocin (STZ)-induced type 1 diabetic rats with/without IGF-1 therapy were used for *in vivo* studies. For *in vitro* studies, DRG neurons from control and STZ-diabetic rats were cultured and treated with/without IGF-1 in the presence or absence of inhibitors or siRNAs.

Results: Dysregulation of mRNAs for IGF-1, AMPKα2, ATP5a1 (subunit of ATPase), and PGC-1β occurred in DRG of diabetic vs. control rats. IGF-1 up-regulated mRNA levels of these genes in cultured DRGs from control or diabetic rats. IGF-1 treatment of DRG cultures significantly ($P < 0.05$) increased phosphorylation of Akt, P70S6K, AMPK and acetyl-CoA carboxylase (ACC). Mitochondrial gene expression and oxygen consumption rate (spare respiratory capacity), ATP production, mtDNA/nDNA ratio and neurite outgrowth were augmented ($P < 0.05$). AMPK inhibitor, Compound C, or AMPKα1-specific siRNA suppressed IGF-1 elevation of mitochondrial function, mtDNA and neurite outgrowth. Diabetic rats treated with IGF-1 exhibited reversal of thermal hypoalgesia and, in a separate study, reversed the deficit in corneal nerve profiles. In diabetic rats, IGF-1 elevated the levels of AMPK and P70S6K phosphorylation, raised Complex IV-MTCO1 and Complex V-ATP5a protein expression, and restored the enzyme activities of Complex IV and I in the DRG. IGF-1 prevented TCA metabolite build-up in nerve.

Conclusions: In DRG neuron cultures IGF-1 signals via AMPK to elevate mitochondrial function and drive axonal outgrowth. We propose that this signaling axis mediates IGF-1-dependent protection from distal dying-back of fibers in diabetic neuropathy.

Keywords IGF-1; AMPK; Axon regeneration; Diabetic neuropathy; Oxygen consumption rate

1. INTRODUCTION

Diabetic sensorimotor polyneuropathy (DSPN) frequently presents with a stocking and glove distribution that is proposed to reflect the dying back of the longest peripheral nerve fibers. Incidence can range from 10% to 90% in diabetic patients, depending on the criteria and methods used to define neuropathy [1]. In humans and animal models of type 1 and type 2 diabetes, the level of available insulin-like growth factor-1 (IGF-1) in serum is substantially decreased, primarily a consequence of suppressed expression in the liver [2–5]. Thus, impaired neurotrophic support by insulin signaling and insulin-like growth factors (IGF-1 and IGF-2) have been proposed to contribute to neurodegeneration in diabetes [6–8]. In addition to a critical role for IGF-1 during nervous system development and early postnatal growth [9], IGF-1 promotes neurite outgrowth in sensory [10,11], motor [12] and sympathetic [9,11] neurons. Further, Schwann cells also require IGF-1 and IGF type 1 receptor signaling for survival, motility, cell proliferation and phenotypic remodeling and myelination [13–16].

[1]Division of Neurodegenerative Disorders, St Boniface Hospital Albrechtsen Research Centre, Winnipeg, MB, Canada [2]Department of Pharmacology and Therapeutics, University of Manitoba, Winnipeg, MB, Canada [3]Department of Pathology, University of California San Diego, La Jolla, CA, USA [4]Department of Human Nutritional Sciences, University of Manitoba, Winnipeg, MB, Canada [5]Canadian Centre for Agri-Food Research in Health and Medicine, St. Boniface Hospital Albrechtsen Research Centre, Winnipeg, Canada [6]Department of Physiology and Pathophysiology, University of Manitoba, Winnipeg, Canada

*Corresponding author. St Boniface Hospital Albrechtsen Research Centre, R4046 - 351 Taché Ave, Winnipeg, Manitoba, R2H 2A6, Canada. E-mail: pfernyhough@sbrc.ca (P. Fernyhough).

Received October 8, 2018 • Revision received November 20, 2018 • Accepted November 23, 2018 • Available online 28 November 2018

https://doi.org/10.1016/j.molmet.2018.11.008

Following peripheral nerve injury, the local or systemic delivery of IGF-1 improves the rate of sciatic nerve regeneration in age matched control or streptozotocin (STZ)-induced type 1 diabetic rats [5,17,18]. Hyperalgesia was also prevented/reversed in STZ-induced diabetic rats treated with IGF-1 [19]. Lumbar intrathecal injection of IGF-1 reversed indices of neuropathy including the deficit in intra-epidermal nerve fiber (IENF) density, sural nerve axonal degeneration, and reduced sensory and motor nerve conduction velocities in STZ-induced type 1 diabetic rats [20,21]. Adenovirus-mediated IGF-1 expression via an intrathecal route or through the liver improved nerve regeneration, myelination, and motor and sensory nerve conduction velocities in mouse models of diabetic neuropathy [22,23]. Finally, IGF binding protein 5, an endogenous inhibitor of IGF-1 action, is up-regulated in sural nerve biopsies from persons with diabetic neuropathy, and its over-expression in transgenic mice induced motor and sensory neuropathy [24]. Thus, there is extensive evidence of the therapeutic potential of IGF-1 in animal models of diabetes. However, less is known about the cellular mechanisms by which IGF promotes neuroprotection in diabetes.

IGF type 1 receptor mobilizes two widely known pathways, the Akt/phosphoinositide-3 kinase (PI-3K) and the mitogen-activated protein (MAP) kinase pathways, mediated by insulin receptor substrate (IRS) 1 and IRS 2 phosphorylation following ligand binding [25,26]. The Akt/PI-3K pathway activates the mammalian target of rapamycin (mTOR) pathway, which directs protein synthesis and cell growth via downstream effectors, P70S6K and 4E-binding protein 1 (4E-BP1) [26]. The MAPK pathway incorporates activation of extracellular signal-regulated kinase (ERK)-1/2 and target transcription factors such as Elk-1 to regulate cell survival [25]. IGF-1 also activates AMP-activated protein kinase (AMPK) during osteoblast differentiation [27]. The AMPK-α subunit is phosphorylated and activated by IGF-1 in an ataxia telangiectasia mutated (ATM)-dependent manner in a human pancreatic cancer cell line [28]. Alternatively, IGF-1 suppresses AMPK activity in vascular smooth muscle cells mediated through Akt1 which phosphorylates an inhibitory site on AMPK at S485 [29]. Any or all of these pathways could be pertinent to the neuroprotective actions of IGF-1 against diabetic neuropathy.

It may be particularly pertinent that IGF-1 activates AMPK as the AMPK/peroxisome proliferator-activated receptor γ co-activator 1-α (AMPK/PGC-1α) energy sensing pathway augments mitochondrial function in a range of cell types [30]. A well-characterized upstream activator of AMPK is Ca^{2+}/calmodulin-dependent protein kinase kinase β (CaMKKβ) [31]. A small range of studies have demonstrated that IGF-1 can regulate cellular metabolism and bioenergetics in neurons and astrocytes and protect against Huntington's disease [32–35]. In human tissues derived from persons with diabetes there is down-regulation of the AMPK/PGC-1α pathway [36,37]. In animal models of DSPN, the levels of expression and activity of AMPK and PGC-1α are also significantly depressed in the dorsal root ganglia (DRG). Under hyperglycemic conditions it has been proposed that nutrient stress triggers this down-regulation of AMPK [38]. However, the mechanistic interactions between IGF-1, AMPK and mitochondrial function are poorly defined and the contribution of impaired IGF-1 signaling and associated pathways to the pathogenesis of DSPN remain to be characterized. We therefore investigated whether exogenous IGF-1 could optimize AMPK activity and mitochondrial function to promote axonal repair in sensory neurons derived from the DRG of rodents with type 1 diabetes and combined this with assessment of the impact of IGF-1 on indices of small sensory fiber neuropathy in two rodent models of type 1 diabetes.

2. MATERIALS AND METHODS

2.1. Induction of type 1 diabetes

Male Sprague-Dawley rats were obtained from a breeding colony at the University of Manitoba at a weight of 201–225 g and maintained 2 per cage on Sani-Chips bedding (P.J. Murphey, Montville, NJ, USA) in a Canadian Council of Animal Care (CCAC)-accredited vivarium under a 12 hr light:dark cycle with free access to diet (5001, LabDiet with fat content of not less than 4.5%, MO, USA) and municipal water. A randomly selected cohort of rats (275–325 g) were made diabetic (non-fasting blood glucose $>$ 19 mmol/l) by a single 90 mg/kg i.p. injection of STZ (Sigma, St. Louis, MO, USA) as previously described [39]. A randomly selected cohort (N = 12) of 3-month STZ-induced diabetic rats received thrice-weekly subcutaneous injections of 20 μg IGF-1 (recombinant human, Preprotech Inc., Rocky Hill, NJ, USA) per rat between 9 AM and 11 AM as previously described [40] for 11 weeks. Fasting blood glucose concentration was monitored half way through the injection period and at study end using an AlphaTRAK glucometer (Abbott Laboratories, Illinois, USA) to ensure that IGF-1 injection did not affect hyperglycemia. At the end of 24 weeks, blood glucose, glycated hemoglobin (HbA1c Multi-test system, HealthCheck Systems, Brooklyn, NY, USA) and body weight were recorded before tissue collection (Supplemental Table 1). No rats died during the study period, no rats required insulin supplementation to offset extreme weight loss, and, at study end, all STZ-injected rats remained hyperglycemic (non-fasting blood glucose $>$ 19 mmol/l). Animal procedures were approved by the University of Manitoba Animal Care Committee and followed CCAC rules.

2.2. Hind paw thermal sensitivity test in adult rats

Hind paw thermal response latencies were measured using a Hargreaves apparatus (UARD, La Jolla, CA, USA) as previously described [41]. Briefly, between 9 AM and 3 PM, rats were placed in plexiglass cubicles on top of the thermal testing system. The heat source was placed below the middle of one of the hind paws and latencies of the paw withdrawal to the heat source were automatically measured. Response latency of each paw was measured three times at 5 min intervals and the mean values were determined.

2.3. Intra-epidermal nerve fiber density in hind paw footpads

The plantar dermis and epidermis of the hind paw were removed and placed in 4% paraformaldehyde. Tissue was coded, processed to paraffin blocks, cut as 6 μm sections, immunostained using an antibody to PGP 9.5 (1:1000, Biogenesis Ltd. Poole, UK) and the number of immunoreactive IENF and sub-epidermal nerve profiles (SNP) per unit length quantified under light microscopy [41].

2.4. Corneal nerve density

Adult (20–30 g) female Swiss Webster mice (Envigo, CA, USA) were maintained 3–4 per cage on TEK-Fresh bedding (7099, Envigo) in an AALAC-accredited vivarium under a 12hr light:dark cycle with free access to diet (5001, LabDiet, MO, USA) and municipal water. A randomly selected cohort of mice was made diabetic (non-fasting blood glucose $>$15 mmol/l) by injection of STZ (75 mg/kg i.p. on 2 consecutive days) following overnight fast. This cohort was maintained untreated for 8 weeks, along with the remaining age- and sex-matched control mice. After 8 weeks of diabetes, the cohort was divided into 2 groups of mice, one of which (N = 10) received daily delivery of IGF-1 to one eye by eye-drop (50 μl of 25 ng/ml solution in 0.9% saline) while the other diabetic group (N = 9) and the control

group (N = 9) received saline vehicle alone. Treatment was given between 8 and 10 am each day to manually restrained unanesthetized animals in their home cage and continued for 4 weeks. No mice died during the study period, and, at study end, all STZ-injected mice remained hyperglycemic (non-fasting blood glucose >15 mmol/l). Corneal nerves of the sub-basal nerve plexus were imaged in isofluorane-anesthetized mice at 3 time points: before onset of diabetes, at week 8 of diabetes, and after 4 weeks of treatment using a Heidelberg Retina Tomograph 3 with Rostock Cornea Module (Heidelberg Engineering, Heidelberg, Germany). Images were collected from randomly selected animals by an investigator unaware of the treatment groups and the image stack from each animal was coded. Nerve occupancy of 5 consecutive images (2 μm intervals) of the cornea between the superficial corneal epithelium and the stroma was calculated using an 8 × 8 grid superimposed on randomized and coded images [42], as described in detail elsewhere [41]. These studies were carried out using protocols approved by the Institutional Animal Care and Use Committee of the University of California, San Diego.

2.5. Adult DRG sensory neuron culture

DRGs were isolated from adult male Sprague-Dawley (300–350 g) rats and dissociated using previously described methods [43]. Neurons were cultured in no-glucose Hams F12 media supplemented with Bottenstein's N2 without insulin (0.1 mg/ml transferrin, 20 nM progesterone, 100 μM putrescine, 30 nM sodium selenite 0.1 mg/ml BSA; all additives were from Sigma, St Louis, MO, USA; culture medium was from Caisson labs, USA). DRG neurons from control rats were cultured in the presence of 5 mM D-glucose and DRG neurons derived from STZ-induced diabetic rats with 25 mM D-glucose. No neurotrophins or insulin was added to any DRG cultures. The following pharmacological inhibitors were used: Compound C, a selective and reversible AMPK inhibitor (Abcam, Cambridge, MA, USA), MK-2206, a highly selective pan-Akt inhibitor (Santa Cruz Biotechnology, Texas, USA), U0126, a selective non-competitive inhibitor of MAP kinase kinase (Abcam, Cambridge, MA, USA), and STO-609, a selective CaMKKβ inhibitor (Santa Cruz Biotechnology, Texas, USA).

2.6. AMPK isoform-specific knockdown

DRG neurons were dissociated and subjected to AMPK isoform-specific knockdown according to the instruction manual of the Amaxa® Rat Neuron Nucleofector Kit (Lonza Inc., Basel, Switzerland). Briefly, the neuron pellet was resuspended at room temperature in 100 μl of Nucleofector® solution with 200 nM siRNA specific to AMPKα1, 5′-CGAGUUGACUGGACAUAAATT-3' (siRNA ID:194424, Thermo Scientific, Pittsburgh, PA, USA), or AMPKα2, 5′-GGUUGACAAUCGGAGCUAUTT-3' (siRNA ID:s134962, Thermo Scientific, Pittsburgh, PA, USA), or a scrambled siRNA (Cat #:4390843, Thermo Scientific, Pittsburgh, PA, USA) as a negative control. The suspension was transferred into a certified cuvette and Nucleofector® program O-003 on Amaxa Nucleofector machine (Lonza Inc., Basel, Switzerland) was used to electroporate/transfect the cells with the corresponding siRNA. Neurons were then plated for further experimentation.

2.7. Luciferase-based ATP assay in DRG culture

To measure ATP production by DRG neurons, Luminescent ATP detection assay kit (ab113849: Abcam, Cambridge, MA, USA) was used. In brief, cultured DRG neurons and an ATP standard dilution series were treated with detergent supplied in the kit and shaken for 5 min. A solution containing D-Luciferin and firefly luciferase were added to the reaction mix and shaken on a plate stirrer for 5 min. After 10 min adaptation to the dark, luminescence from luciferase activity was measured and recorded using the Glomax-multi detection system (Promega, Wisconsin, USA). A standard curve was plotted and luminescent units from each sample were interpolated in order to calculate the absolute ATP concentration per mg of total protein lysate.

2.8. Quantitative Western blotting

Rat DRG neurons were harvested from culture or isolated intact from adult rats and then homogenized in ice-cold RIPA buffer containing: 25 mM Tris pH = 8, 150 mM NaCl, 0.1% SDS, 0.5% sodium deoxycholate, 1% Triton X-100 and protease phosphatase inhibitors. Proteins (2–20 μg total protein/lane) were resolved and separated via 10% sodium dodecyl sulphate-polyacrylamide gel electrophoresis (SDS-PAGE). The proteins were subsequently transferred to a nitrocellulose membrane (Bio-Rad, CA, USA) using Trans-Blot Turbo Transfer System (Bio-Rad, CA, USA) and immunoblotted with specific antibodies against pP70S6K T389 (1:1000, Cell Signaling Technology, Massachussetts, USA), pAkt S473 (1:1000, Santa Cruz Biotechnology, Texas, USA), total Akt (1:1000, Abcam, Cambridge, MA, USA), pAMPK T172 (1:1000, Cell Signaling Technology, Massachussetts, USA), total AMPK (1:800, Santa Cruz Biotechnology, Texas, USA), total OXPHOS (1:2000, MitoSciences, Abcam, Cambridge, MA, USA), PGC-1α (1:1000, Abcam), pACC S79 (1:1000, Cell Signaling Technology, Massachussetts, USA) and total ERK (1:1000, Santa Cruz Biotechnology, Texas, USA). Of note, total protein bands were captured by chemiluminescent imaging of the blot after gel activation (TGX Stain-Free™ FastCast Acrylamide Solutions, Bio-Rad, CA, USA) in addition to the use of T-ERK levels for target protein normalization (to adjust for loading). The secondary antibodies were HRP-conjugated goat anti-rabbit IgG (H + L) or goat anti-mouse IgG (H + L) from Jackson ImmunoResearch Laboratories, PA, USA. The blots were incubated in ECL Advance (GE Healthcare) and imaged using a Bio-Rad ChemiDoc image analyzer (Bio-Rad, CA, USA).

2.9. Real-time PCR array

RNA was extracted from cultured neurons or previously frozen tissue samples using TRIzol® Reagent (Invitrogen, California, USA). Complementary DNA (cDNA) was synthesized from RNA samples by using the iScript™ gDNA Clear cDNA Synthesis Kit (Bio-Rad, CA, USA) according to the manufacturer's instructions. Quantitative real-time PCR (QRT-PCR) was performed using iQ™ SYBR® Green Supermix (Bio-Rad, CA, USA) or Bright Green Master mix (Abmgood Co., Richmond, Canada) compatible with the iQ5 Cycler machine (Bio-Rad, CA, USA). The ΔΔCt method was used to quantify gene expression. The mRNA level of GAPDH and B2m were used for normalization.

2.10. Mitochondrial DNA/Nuclear DNA (mtDNA/nDNA) ratio

Total DNA was extracted from DRGs by using a modified salting-out DNA extraction method and subjected to QRT-PCR using iQ™ SYBR® Green Supermix (Bio-Rad, CA, USA). To calculate mtDNA/nDNA ratio, we designed primers specific to D-loop regions on rat mitochondrial DNA, and to ApoB and B2m genes on the rat nuclear DNA. PCR product size and specificity were validated using melt curve and 4% agarose gel (Supplementary Figure 1A and B).

2.11. Mitochondrial respiration in cultured neurons

An XF24 analyzer (Seahorse Biosciences, Billerica, MA, USA) was used to measure the basal level of mitochondrial oxygen consumption rate (OCR), the maximal respiration, the spare respiratory capacity and the coupling efficiency. In short, DRG culture medium was changed 1 h before the assay to unbuffered DMEM (Dulbecco's modified Eagle's medium, pH 7.4) supplemented with 1 mM sodium pyruvate, and

5 mM D-glucose. For diabetic rat DRG cultures, 25 mM D-glucose was used. Four mitochondrial complex inhibitors including oligomycin (1 μM), FCCP (1 μM) and rotenone (1 μM) + antimycin A (1 μM) were injected sequentially through ports in the Seahorse Flux Pak cartridges. Oligomycin acts as an irreversible ATP synthase inhibitor, FCCP as an uncoupler, rotenone as Complex I inhibitor, and antimycin A as an inhibitor of Complex III of the mitochondrial electron transport system. After OCR measurement, cells were subjected to protein assay (DC protein assay, BioRad, USA) for normalization purpose and, in some cases, Western blotting. OCR measures from each well were normalized to total protein levels and are presented as pmoles/min/mg protein.

2.12. Neurite outgrowth in DRG cultures

DRG neurons were cultured on glass coverslips. Then, they were fixed with 4% paraformaldehyde in PBS (pH 7.4) for 15 min at room temperature then permeabilized with 0.3% Triton X-100 in PBS for 5 min. Neurons were incubated with 5% BSA in PBS for 1 h and with neuron-specific β-tubulin III antibody (1:1000; from Sigma, St Louis, MO, USA) overnight. Following three washes with PBS, cells were incubated with Cy3-conjugated secondary antibody (1:1000, Jackson ImmunoResearch Laboratories Inc., PA, USA) for 1 h at room temperature. Coverslips were mounted on slides using VECTASHIELD antifade mounting medium with DAPI (Vectorlabs, Inc., CA, USA) and imaged using a Carl Zeiss Axioscope-2 upright fluorescence microscope equipped with AxioVision3 software. The fluorescent signal was collected as total pixel area for neurites and was measured by the high throughput NeurphologyJ plugin in ImageJ software after image enhancement. Total pixel area was normalized to number of cell bodies to calculate total neurite outgrowth per neuron.

2.13. Mitochondrial isolation and enzymatic activity of respiratory complexes I and IV in DRG

DRG tissues were homogenized in mitochondrial isolation buffer (MIB) consisting of 70 mM sucrose, 210 mM mannitol, 5.0 mM HEPES PH 7.2, 1.0 mM EGTA, and 0.5% (w/v) fatty acid free BSA using a Dounce homogenizer. Supernatant from a double centrifugation of the tissue at 800 g for 15 min was centrifuged twice at 8000 g for 10 min and the pellet subjected to enzymatic activity assays. Enzymatic activity of cytochrome *c* oxidase (a subunit of Complex IV of the mitochondrial electron transport system) was measured by a temperature controlled Ultrospec 2100 UV—visible spectrophotometer equipped with Biochrom Swift II software (Biopharmacia Biotech). Briefly, 0.02% lauryl maltoside was mixed with 10 μg purified mitochondria and incubated for 1 min before addition of 40 μM reduced cytochrome *c* and 50 mM KPi to the mixture. The resulting absorbance decrease of reduced cytochrome *c* at 550 nm was monitored for 2 min [44]. Enzymatic activity of mitochondrial Complex I was measured according to the instruction manual of the kit (Cat #:K968-100, BioVision, California, USA). Data was collected at 5 min by reading the absorbance of the mixture (10 μg mitochondria, Complex I assay buffer, Decylubiquinone and Complex I dye) at 600 nm using a Ultrospec 2100 UV-visible spectrophotometer and the kinetic reduction of Complex I dye was calculated as Complex I activity.

2.14. Metabolomic analysis of nerve

The tibial nerve tissue from rats was utilized for biochemical analyses. The nerve (10—30 mg) was homogenized with 500 μl ultrapure water (Milli-Q H2O, EMDMillipore, Billerica, USA) using a bead homogenizer (Omni Bead Ruptor 24, OMNI, USA). The same volume of methanol (500 μl) was added to the homogenized tissue, and the mixture was vortexed, sonicated and centrifuged at 10500 g for 5 min. The supernatant was dried under a gentle flow of nitrogen, and reconstituted in 100 μl deionized water:methanol (1:1) containing 150 ng of each of the following internal standards: L-Tryptophan-d5, L-Valine-d8, L-Alanine-d4, L-Leucine-d10, Citric Acid-d4 and D-Fructose (all from Sigma, USA). Metabolomics analysis was performed on a 1290 Infinity Agilent high performance liquid chromatography (HPLC) system coupled to a 6538 UHD Accurate Quadrupole time-of-flight liquid chromatography/mass spectrometry (Q-TOF LC/MS) from Agilent Technologies (Santa Clara, CA, USA) equipped with a dual electrospray ionization source as described elsewhere [45]. A Zorbax SB-Aq 4.6 × 100 mm, 1.8 U, 600 bar column (Agilent Technologies) was used to separate metabolites while the column temperature was maintained at 55 °C. In brief, a sample size of 2 μl was injected into the Zorbax column by maintaining the HPLC flow rate at 0.6 ml/min. The mass detection was operated using dual electrospray with reference ions of *m/z* 121.050873 and 922.009798 for positive mode, and *m/z* 119.03632 and 980.016375 for negative mode. Targeted MS/MS mode was used to identify potential biomarkers using Agilent MassHunter Qualitative (MHQ, B.07) and Mass Profiler Professional (MPP, 12.6.1). The Molecular Feature Extraction (MFE) parameters were set to allow the extraction of detected features satisfying absolute abundances of more than 4000 counts. The data were normalized using a percentile shift algorithm set to 75 and were adjusted to the baseline values of the median of all samples.

2.15. Statistical analysis

Data were analyzed using two-tailed Student's t-tests or one-way ANOVA followed by Tukey's or Dunnett's post hoc tests, as appropriate and indicated (GraphPad Prism 7, GraphPad Software). A P value < 0.05 was considered to be significant. The HeatMap was made using GraphPad (GraphPad Prism 7, GraphPad Software). The metabolomics data were analyzed using One Way ANOVA ($P < 0.05$) followed by Benjamini-Hochberg multiple testing corrections (Mass Professional Profiler 12.6.1 and XLSTAT).

3. RESULTS

3.1. IGF-1 enhances mitochondrial respiration and ATP production in cultured DRG neurons from control and diabetic rats

DRG neurons derived from control rats were cultured and treated with IGF-1 (10 nM) for 2—24 h. This concentration of IGF-1 does not cross-occupy the insulin receptor in neurons [46]. Mitochondrial oxygen consumption rate (OCR) was enhanced at 24 h but not at 2 h or 6 h (Figure 1A). Bioenergetic parameters of maximal respiration and spare respiratory capacity were significantly ($P < 0.05$ and $P < 0.01$, respectively) increased 24 h after IGF-1 treatment (Figure 1B). Nevertheless, IGF-1 did not affect the corrected oligomycin-insensitive mitochondrial respiration rate (proton leak) (Supplementary Figure 2). IGF-1 treatment of DRG neurons derived from age-matched diabetic rats showed up-regulation of mitochondrial maximal respiration at 2 h and 24 h treatment. Spare respiratory capacity was elevated at least 3-fold, although not reaching statistical significance, and respiratory control ratio was significantly increased at 2 h and 24 h of IGF-1 treatment (Figure 1C). To confirm that the mitochondrial OCR was reflected by similar alterations in cellular ATP production, DRG neurons from control rats were treated with various doses of IGF-1 for 24 h and ATP production was measured in live cells. At doses of 1, 10, and 100 nM, but not 0.1 nM, IGF-1 augmented ATP production ($P < 0.05$) (Figure 1D).

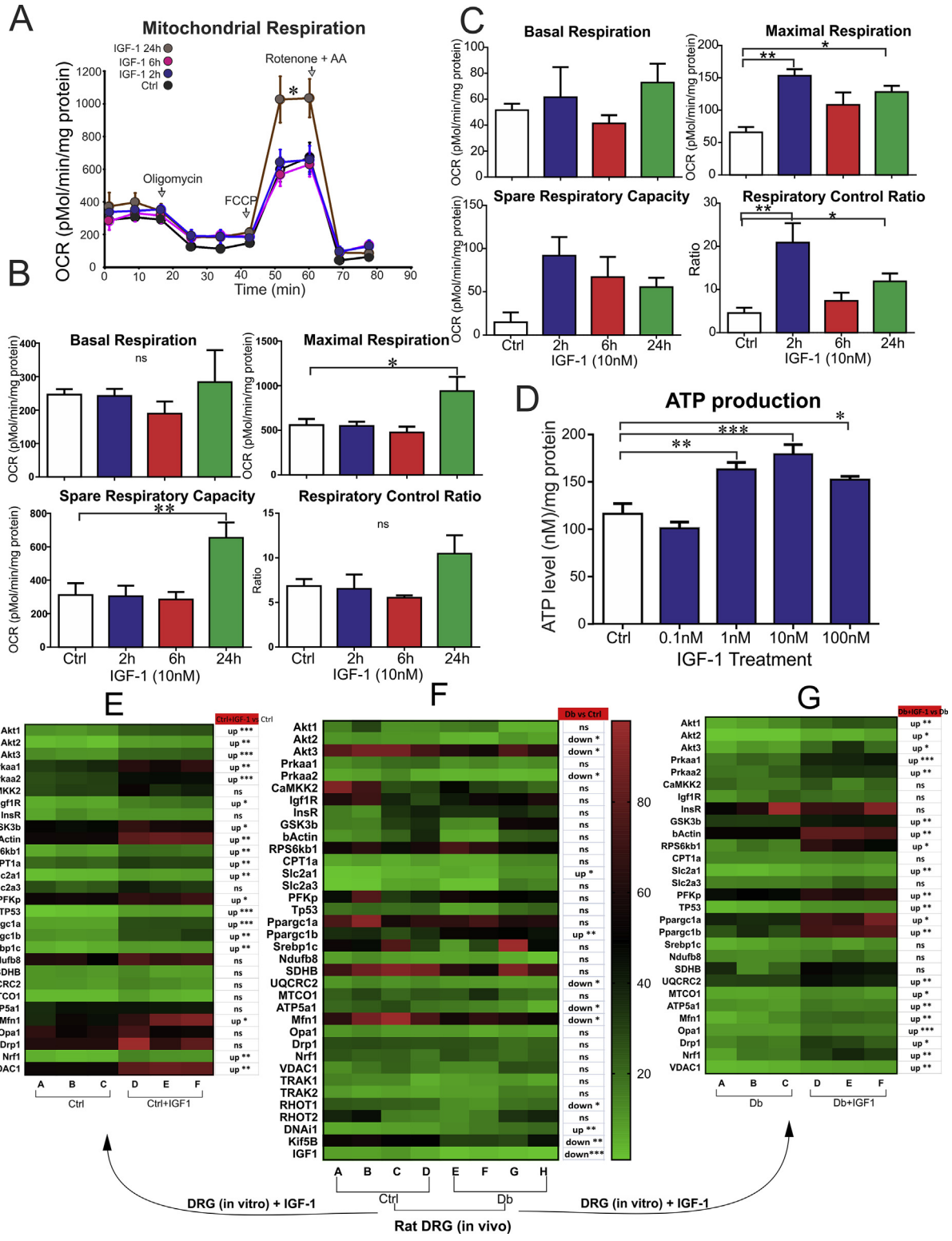

Figure 1: Mitochondrial function-related genes are dysregulated in DRG neurons from diabetic rats, and exogenous IGF-1 modulates selective transcripts and upregulates mitochondrial respiration and ATP production in cultured adult sensory neurons. DRG neurons derived from (A, B, D) adult control or (C) diabetic rats were treated with/without IGF-1 for 2–24 h. In (A, B, C) the culture plate was then inserted into the Seahorse XF24 Analyzer and oligomycin, FCCP and rotenone + AA (antimycin A) added sequentially. In (D) ATP concentration was calculated from proportional luminescent reads by a GloMax®-Multi Detection System. Data were normalized to protein concentration units per well prior to statistical analysis. Real-time PCR array derived mRNA levels for (F) DRG tissues or (E and G) cultured DRG neurons treated with IGF-1 for 6 h, from control (ctrl) and diabetic (Db) rats. All mRNA levels were calculated relative to *GAPDH* or *B2m* mRNA levels using the ΔΔ Ct method. Data are mean ± SEM of N = 3–5 replicates; * = $p < 0.05$ or ** = $p < 0.01$ or *** = $p < 0.001$ or **** = $p < 0.0001$; analyzed by unpaired Student's t-test or one-way ANOVA with Dunnett's *post-hoc* test.

3.2. Genes linked to mitochondrial function were dysregulated in DRGs from control vs. diabetic rats and *in vitro* were up-regulated after IGF-1 treatment

The mRNA levels of a number of genes downstream of IGF-1 signaling that are linked to mitochondrial function, including Akt2, Akt3, AMPKα2, UQCRC2, ATP5a1, MFN1, RHOT1, IGF-1, and Kif5B, were down-regulated in DRG of diabetic rats when compared to control rats ($P < 0.05$) (Figure 1F). Some mRNAs including those for Slc2a1 (Glut1), Ppargc1β (PGC-1β) and DNAi1 were up-regulated in DRGs of diabetic rats (Figure 1F). IGF-1 (10 nM) treatment of cultured DRGs from control rats for 6 h up-regulated Akt1, Akt2, Akt3, AMPKα1, AMPKα2, IGF-1R, GSK3β, β-actin, RPS6Kb1 (P70S6K), CPT1a, Glut1, PFKp, P53, Ppargc1α (PGC-1α), PGC-1β, Srebp1c, MFN1, Nrf1, and VDAC1 mRNA levels when compared to untreated DRG neurons ($P < 0.05$) (Figure 1E). DRGs derived from diabetic rats and treated *in vitro* with IGF-1 showed a significant ($P < 0.05$) up-regulation in mRNA levels of Akt1, Akt2, Akt3, AMPKα1, AMPKα2, GSK3 β, β-actin, P70S6K, Glut1, PFKp, P53, PGC-1α, PGC-1β, UQCRC2, MTCO1, ATP5a1, MFN1, Opa1, Drp1, Nrf1, and VDAC1 genes vs. untreated cultured DRG neurons (Figure 1G).

3.3. IGF-1 augments AMPK, Akt, ACC phosphorylation, and respiratory protein expression in cultured neurons from control rats

DRG neurons from age matched control rats treated with 10 nM IGF-1 exhibited elevated phosphorylation of Akt (at S473) within 15 min (Figure 2A,B) and at 2 h this was associated with enhanced phosphorylation of pP70S6K (a downstream substrate for P-Akt) (Supplementary Figure 3D). IGF-1 elevated phosphorylation of AMPK at

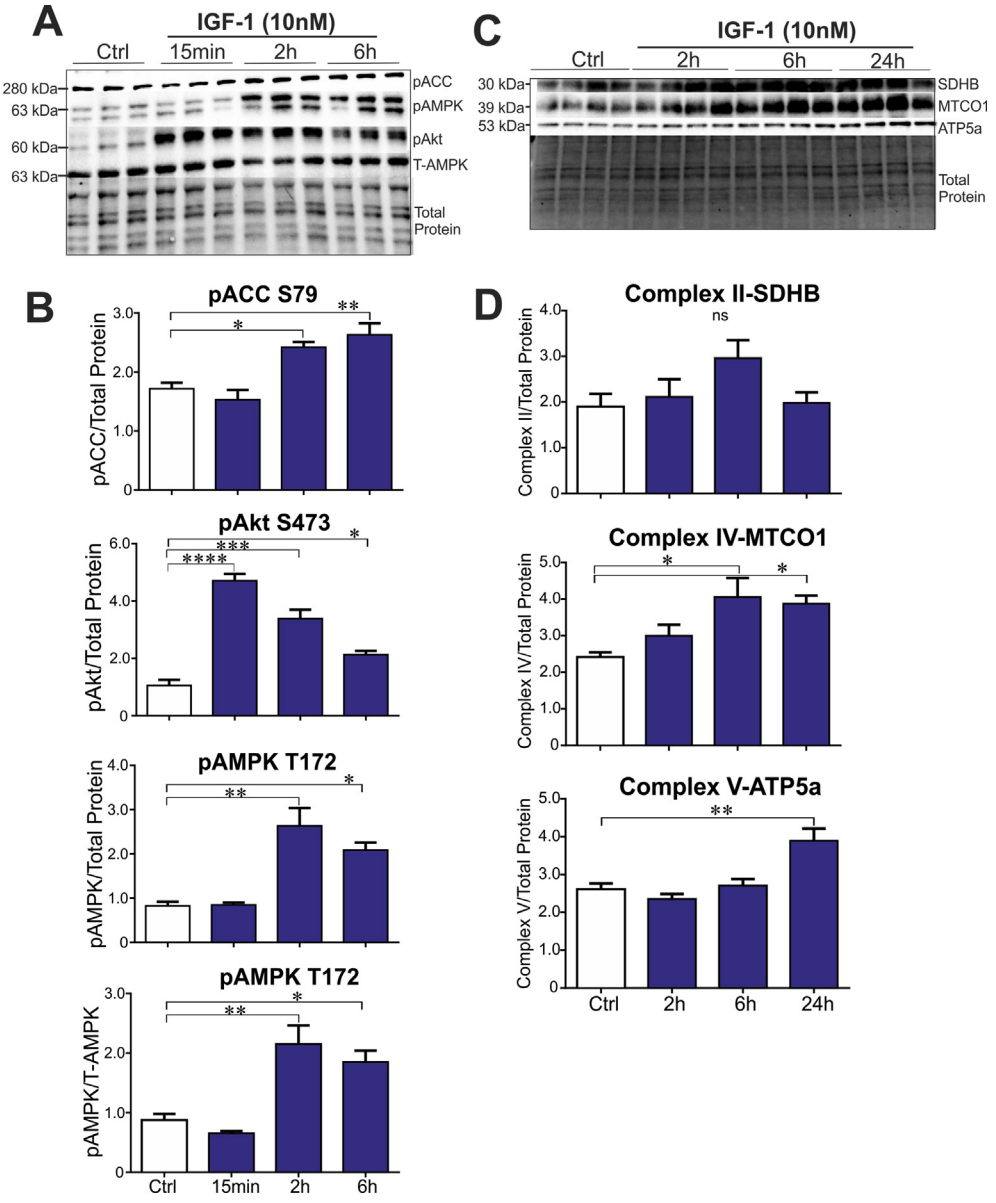

Figure 2: IGF-1 treatment increases Akt and AMPK phosphorylation, and the expression of electron transport chain proteins. DRG neurons derived from adult control rats were treated with/without 10 nM IGF-1 for (A, B) 15 min-6 h or (C, D) 2–24 h and lysates subjected to Western blotting. Specific proteins from each respiratory Complex were quantified and expressed relative to total protein. Complexes I-NDUFB8 and III-UQCRC2 subunit proteins were not detectable. Data are mean ± SEM of N = 3–4 replicates; * = $p < 0.05$ or ** = $p < 0.01$ or *** = $p < 0.001$ or **** = $p < 0.0001$ vs ctrl by one-way ANOVA with Dunnett's *post-hoc* test.

T172 and also its phosphorylation target acetyl-Co-A carboxylase (P-ACC) at 2 h and 6 h (Figure 2A,B). These effects were dose dependent; with 10 nM IGF-1 giving the highest P-AMPK and P-ACC levels, whereas 100 nM induced the highest activation of Akt (Supplementary Figure 3A and B). Treatment for up to 24 h with 10 nM IGF-1 up-regulated the total protein levels for AMPK and Akt (Supplementary Figure 3C). The stimulatory effect of IGF-1 on total protein expression levels for AMPK and Akt at 6 h and 24 h was the reason we normalized all data to total protein levels. Mitochondrial OXPHOS proteins, components of the electron transport system (ETS), including Complex components IV-MTCO1 and V-ATP5a were significantly elevated after 6 h—24 h of IGF-1 treatment (Figure 2C,D). IGF-1 also elevated these same Complex proteins and Complex II-SDHB in DRG neuron cultures derived from STZ-induced type 1 diabetic rats (Supplementary Figure 4A and B). Overall, the impact of IGF-1 on the level of expression of these respiratory chain proteins was greater in the diabetic cultures compared with control age-matched cultures.

3.4. AMPK inhibitor, AMPKα1 knockdown, and Akt inhibitor suppress the IGF-1 induced up-regulation of mitochondrial function in DRG neurons from control rats

The stimulatory effect of IGF-1 on AMPK activity and respiratory chain protein expression provided a good rationale to study putative effects on mitochondrial function. To identify the signaling pathway utilized by IGF-1 to modulate mitochondrial function, DRG neurons from control rats were cultured and pretreated with 1 μM compound C (AMPK inhibitor), MK-2206 (Akt inhibitor) or STO-609 (CaMKKβ inhibitor) 2 h prior to 10 nM IGF-1 treatment for 24 h. Seahorse XF24 assay for OCR revealed that IGF-1 up-regulated mitochondrial function with respect to augmented maximal respiration and spare respiratory capacity (Figure 3A,B). This effect was completely suppressed by the AMPK inhibitor and partially suppressed by the Akt inhibitor (Figure 3A,B). The CaMKKβ inhibitor STO-609 also prevented induction of mitochondrial function by IGF-1 but this effect did not reach statistical significance (Figure 3A,B). To specifically knockdown isoforms of AMPK, DRG

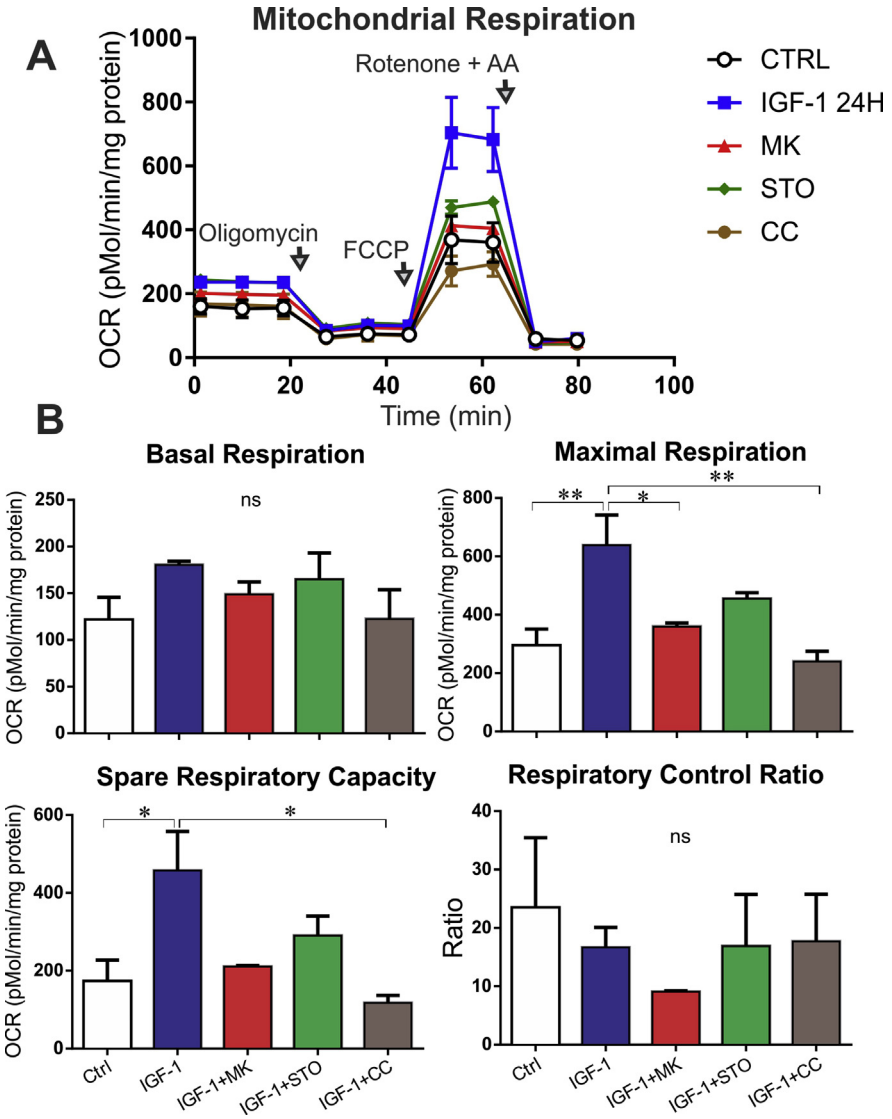

Figure 3: Compound C (AMPK inhibitor) suppresses the IGF-1 upregulation of mitochondrial respiration. (A, B) DRG neurons derived from control rats were cultured, pretreated with inhibitors 2 h prior to IGF-1 treatment and maintained for 24 h. Mitochondrial respiration was measured using Seahorse XF24 Analyzer. CC (compound C, 1 μM): AMPK inhibitor, MK (MK-2206, 1 μM): Akt inhibitor and STO (STO-609, 1 μM): CaMKKβ inhibitor. Data were normalized to protein concentration units per well prior to statistical analysis. Data are mean ± SEM of N = 3—5 replicates; * = $p < 0.05$ or ** = $p < 0.01$; analyzed by one-way ANOVA with Tukey's *post-hoc* test.

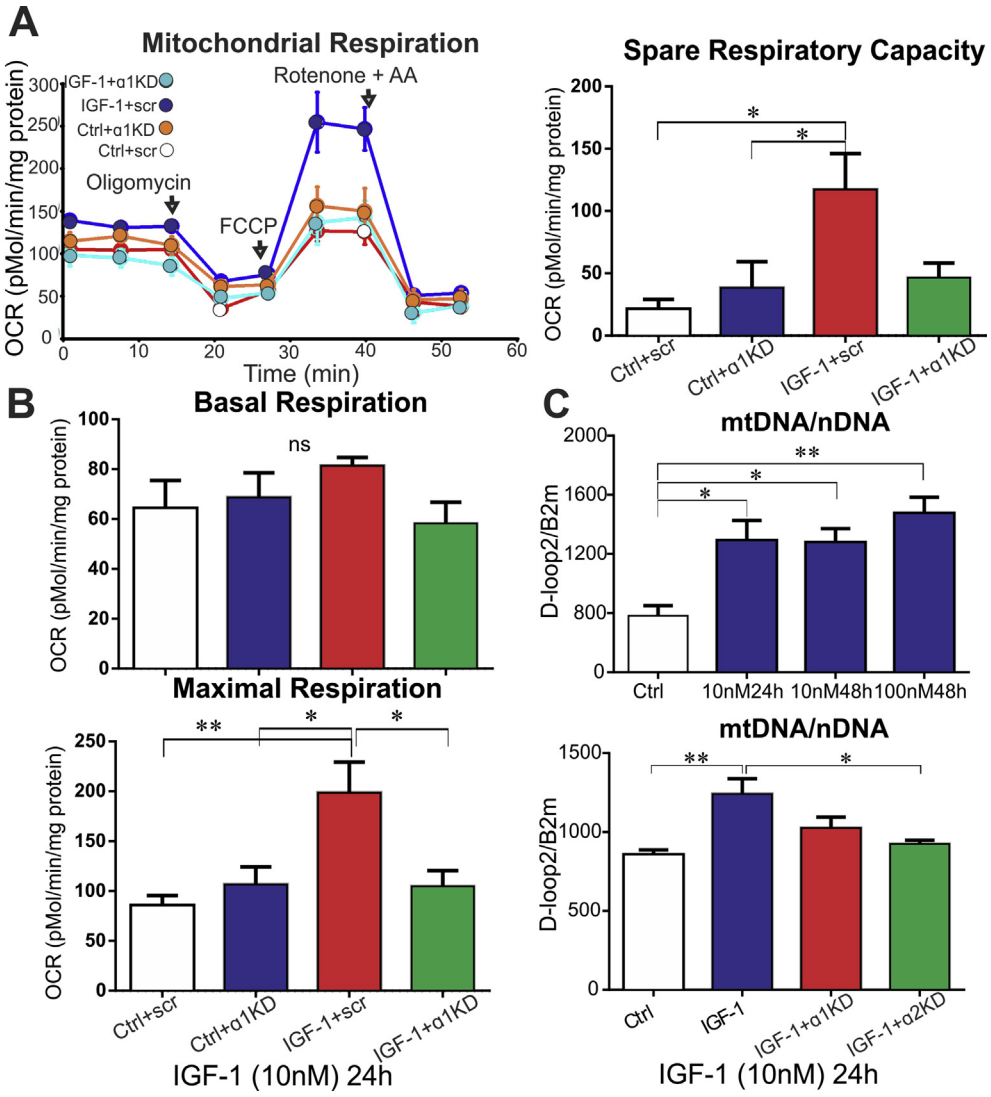

Figure 4: IGF-1 acts through AMPKα1 and α2 to augment mitochondrial function and mtDNA copy number. (A, B) DRG neurons derived from adult control rats were transfected with AMPKα1-or α2-specific siRNAs, cultured for 24 h and treated with/without 10 nM IGF-1 for another 24 h. Mitochondrial respiration was measured using Seahorse XF24 Analyzer. Data were normalized to protein concentration units per well prior to statistical analysis. (C) DRG neurons from control rats were cultured and treated with different IGF-1 doses (10 nM and 100 nM) for 24—48 or transfected with AMPKα1-or α2-specific siRNAs, cultured for 24 h and treated with/without 10 nM IGF-1 for another 24 h mtDNA/nDNA ratio was analyzed using Real-Time PCR and calculated using the ΔΔCt method. Data are mean ± SEM of N = 3—5 replicates; * = $p < 0.05$ or ** = $p < 0.01$; analyzed by one-way ANOVA with Tukey's or Dunnett's *post-hoc* test.

neurons were also transfected with siRNAs specific to AMPKα1 or AMPKα2 (and in combination) for 24 h prior to IGF-1 treatment for another 24 h. AMPK knockdown efficiencies were 75—80% for the specific isoform mRNAs and 73% for the total AMPK protein when both siRNAs were combined (Supplementary Figure 5A—C). 2D gel electrophoresis revealed that the isoforms of AMPKα1 (mw 63.97 kDa) and AMPKα2 (mw 62.26 kDa) could be visualized (Supplementary Figure 5D). Supplementary Figure 5D and E shows that siRNA knockdown for each isoform was relatively specific. SiRNA to AMPKα1 caused a 77% knockdown and only reduced AMPKα2 by 16% (Supplementary Figure 5F). For siRNA to AMPKα2, the values were 61% for its own isoform and 16% for the AMPKα1. SDS-PAGE revealed effective knockdown of phosphorylated AMPK and its target P-ACC with the combined siRNAs in the presence/absence of IGF-1 for 24 h (Supplementary Figure 6A). Under the same experimental conditions siRNA to AMPKα1 blocked phosphorylated AMPK. However, its target P-ACC was not significantly affected (Supplementary Figure 6B). With the same experimental paradigm OCR measurements showed suppression of IGF-1-driven up-regulation of maximal respiration and spare respiratory capacity in neurons treated with AMPKα1 siRNA (Figure 4A,B) and AMPKα1α2 siRNAs combined (data not shown), but not with siRNA to AMPKα2 (Supplementary Figure 7A—D).

3.5. AMPK knockdown and Akt inhibitor impede IGF-1 enhancement of neurite outgrowth and mtDNA copy number in DRG cultures from control rats

To investigate the inhibitory effect of AMPK on mitochondrial DNA copy number and neurite outgrowth, DRG cultures derived from control rats were transfected with siRNA to AMPKα1 or α2 and treated with IGF-1. IGF-1 (10 nM or 100 nM) significantly ($P < 0.05$) increased mtDNA copy number after 24 h and 48 h (Figure 4C). This effect of IGF-1 on mtDNA was significantly suppressed following treatment with siRNA to

AMPKα2 (Figure 4C). Knockdown of either AMPKα1 or AMPKα2 isoforms also prevented the IGF-1 enhancement of neurite outgrowth (Figure 5A). In a complementary experiment, neurite outgrowth was enhanced by IGF-1 treatment ($P < 0.01$) and pretreatment with Akt inhibitor or AMPK inhibitor Compound C suppressed this neuritogenic effect of IGF-1 (Figure 5B).

3.6. Topical IGF-1 to the eye of diabetic mice reversed the loss of corneal nerve profiles

To address whether the relatively rapid effects of IGF-1 on regulation of mitochondrial respiration and neurite outgrowth from adult sensory neurons *in vitro* predict neurotrophic and neuroprotective properties *in vivo*, we delivered IGF-1 topically to the eye of STZ-induced diabetic mice daily for 4 weeks, following 8 weeks of diabetes. Nerve density of the sub-basal nerve plexus was measured iteratively by corneal confocal microscopy across the study period. Nerve density did not change over the 12-week study period in control mice (Figure 5C–D). Eight weeks of diabetes induced a mild reduction in nerve density that progressed in the subsequent 4 weeks. Initiation of topical IGF-1 treatment prevented this progression such that by the end of the study the vehicle-treated diabetic group had values that were significantly ($P < 0.05$) lower than the IGF-1 treated group.

3.7. IGF-1 therapy reverses thermal hypoalgesia and corrects impaired activities of mitochondrial Complexes I and IV in DRG of diabetic rats

Age-matched control and STZ-induced diabetic rats were maintained for 3 months; then, a cohort of diabetic rats received injections of human recombinant IGF-1 (20 μg/rat per day s.c.) for the final 11 weeks (Figure 6A). Body weight, blood glucose, and glycated hemoglobin values were not any different between untreated and IGF-1-treated diabetic rats (Supplemental Table 1). Thermal testing on the hind paw was performed at three time points and revealed development of hypoalgesia in diabetic rats and significant improvement in the IGF-1-treated diabetic rats at the end of study (Figure 6A). Analysis of IENF density and SNP levels in the hind paw revealed no significant loss of fibers at the end of this study and no effect of IGF-1 treatment on IENF whereas a significant rise in SNP profiles was observed compared to control rats (Figure 6B). Mitochondria isolated from DRGs of diabetic rats exhibited depressed activity levels of mitochondrial Complexes I and IV compared with age matched control and these activities were significantly elevated by IGF-1 therapy (Figure 6C).

3.8. IGF-1 therapy increases the expression of PGC-1α and respiratory chain proteins and up-regulates AMPK, Akt, and P70S6K phosphorylation in DRG of diabetic rats

Due to low tissue availability, each animal group was divided into different sub-groups to perform Western blotting, enzymatic assay, and mRNA measurements on DRGs. Levels of expression of mitochondrial Complex IV-MTCO1 and Complex V-ATP5a, and PGC-1α proteins were suppressed in DRGs derived from diabetic rats by approximately 40% and these deficits were prevented by IGF-1 therapy (Figure 7A). IGF-I therapy also significantly increased the phosphorylation of critical effector proteins upstream of mitochondria including AMPK and P70S6K compared to both control and untreated diabetic rats, while a trend of elevated Akt activation was also observed ($P = 0.08$ vs. control: Figure 7B). It should be noted, that only a partial depression of P-AMPK and P-P70S6K levels were observed in DRGs of the diabetic group versus age-matched control in this study. Consistent with Western blotting data, mRNA levels of AMPKα2 isoform, Complex III-UQCRC2, and Nrf-1 were restored in diabetic rat DRGs after IGF-I therapy (Supplementary Figure 8). AMPKα1, Akt2 and Akt3 mRNAs were not significantly different between groups (Supplementary Figure 8).

3.9. IGF-1 therapy reinstates components of the Krebs cycle, amino acid metabolism, ketosis, and oxidant status but does not correct aberrant glucose metabolism in tibial nerve of diabetic rats

A targeted metabolomics approach was used to monitor 35 selected metabolites (Supplemental Table 2) related to energy generation by mitochondrial function, carbohydrate metabolism and protein metabolism, as recently reported [47]. A total of 13 metabolites were significantly different and exhibited a similar trend between the 3 groups (Figure 8A). The metabolomics analysis of tibial nerve tissues showed that Krebs cycle intermediates including fumaric acid, succinic acid, malic acid and citric acid, and free amino acids or fragmented peptides such as leucine, aspartic acid, and Ala-Cys-Asp, were significantly ($P < 0.05$) up-regulated in nerves of diabetic rats and were returned to the normal range with IGF-1 therapy (Figure 8A). IGF-1 injections did not correct the levels of sorbitol, glucose and myoinositol 4-phosphate, which all represent aberrant glucose metabolism (Figure 8A–B), indicating that IGF-1 did not alter glucose uptake or metabolism within the local environment of the nerve. However, diabetes-induced elevation of oxidized glutathione and ketone bodies including β-hydroxy butyric acid in nerve was reduced by IGF-1 treatment of diabetic animals (Figure 8A). Other metabolites such as isocitrate (TCA metabolite), homoserine (amino acid precursor), and acryloylglycine (fatty acid metabolism) did not differ or show any consistent trends between groups (Supplemental Table 2). The Krebs cycle metabolites, free amino acids, ketone bodies, and oxidized glutathione levels showed similar trends, as illustrated for citric and aspartic acid (Figure 8C–D).

4. DISCUSSION

We demonstrate for the first time that IGF-1 activates and up-regulates AMPK to augment mitochondrial function, ATP production, mtDNA copy number, and expression of ETS proteins in cultured rat DRG neurons. IGF-1 utilizes this AMPK pathway and, possibly in parallel, the Akt pathway to drive axonal outgrowth. Further, we show that IGF-1 therapy prevented diabetes-induced progressive loss of sensory nerves in the cornea and ameliorated paw thermal hypoalgesia. Correction of these clinically relevant endpoints was associated with suppression of build-up of TCA intermediates in nerve and optimization of mitochondrial phenotype in the DRG of type 1 diabetic rats. The stimulatory effect of IGF-1 upon mitochondrial oxygen consumption rate can be explained by signaling via the AMPKα1 isoform. The elevation in mtDNA copy number revealed the involvement of AMPKα2 isoform downstream from IGF-1 signaling.

For more than two decades, a variety of studies have demonstrated that IGF-1 promotes neurite outgrowth and protects from multiple functional and structural indices of diabetic neuropathy in animal models [2,9,10]. The emergence of corneal confocal microscopy as a technique to visualize human sensory nerves *in situ* has provided a non-invasive and sensitive biomarker of DSPN that offers the opportunity to track progression of neuropathy and efficacy of therapeutic interventions [48]. Diabetic rodents also develop loss of corneal nerves [42,49] and topical delivery of potential therapies to the eye provides a useful translational model that bridges *in vitro* and traditional *in vivo* therapeutic studies. Our demonstration that topical delivery of IGF-1 prevented progressive corneal nerve loss in diabetic mice provides *in vivo* validation of our *in vitro* model using adult sensory neuron

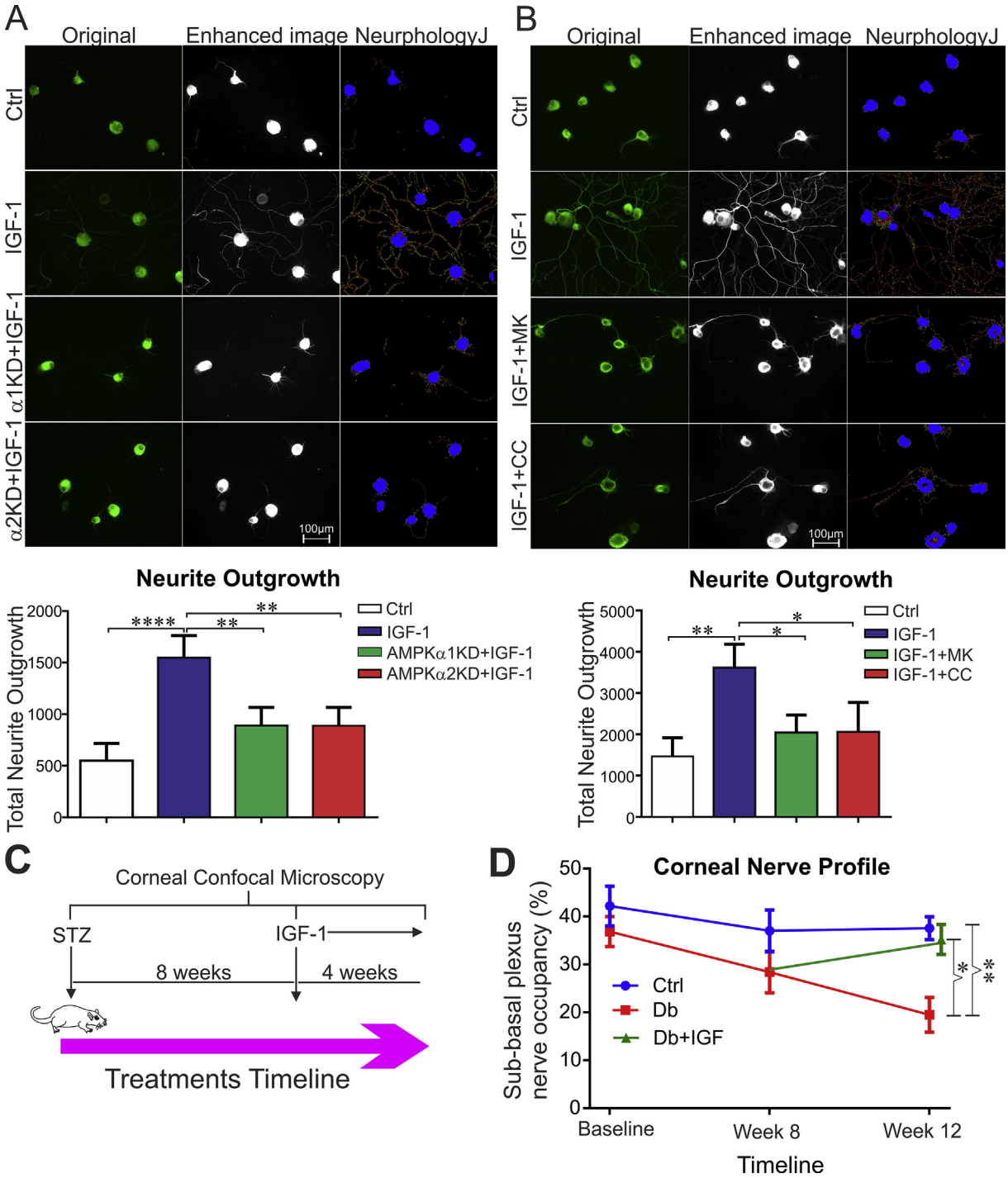

Figure 5: AMPK and Akt inhibition suppresses the axonal regeneration triggered by IGF-I in cultured DRGs from rats and topical IGF-1 prevents progressive loss of corneal nerves in diabetic mice. DRG neurons derived from adult control rats were (A) transfected with AMPKα1-or α2-specific siRNAs, cultured for 24 h or (B) pretreated with inhibitors for 2 h and treated with/without 10 nM IGF-1 for another 24 h. β-tubulin III immunostaining was used to stain sensory neurons and NeurphologyJ was used for automated neurite tracing. CC (compound C, 1 μM): AMPK inhibitor and MK (MK-2206, 1 μM): Akt inhibitor. Total neurite outgrowth data is presented relative to neuron number. Data are mean ± SEM of N = 4 replicates; * = $p < 0.05$ or ** = $p < 0.01$ or **** = $p < 0.0001$; analyzed by one-way ANOVA with Tukey's *post-hoc* test. (C) Reveals the time line for the topical delivery of IGF-1 to the eye of STZ-induced diabetic mice. (D) Line chart showing nerve density (as % occupancy) in the sub-basal nerve plexus of control (blue line), diabetic (STZ: red line) and IGF-1 treated diabetic (STZ + IGF-1; green line) mice at 0, 8 and 12 weeks of diabetes. IGF-1 treatment was initiated at 8 weeks. Data are group mean ± SEM of N = 9–10/group. At week 12 * = $p < 0.05$ for Db vs Db + IGF-1 group and **p=<0.01 for Db vs age matched control group by two-way ANOVA with Tukey's *post-hoc* test.

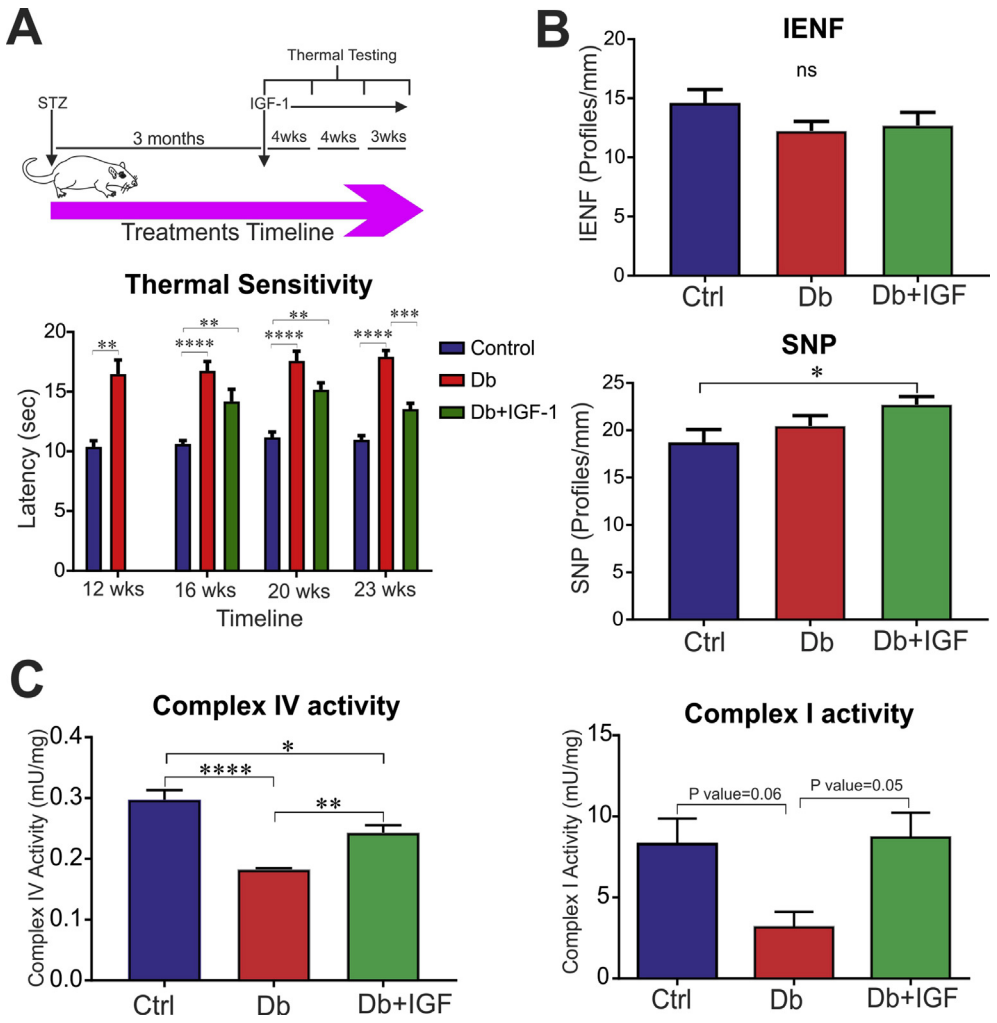

Figure 6: IGF-1 therapy restored the activity of Complexes I and IV and prevented thermal hypoalgesia in diabetic rats. Control (ctrl), diabetic (Db) and IGF-1-treated diabetic (Db + IGF-1) rats were tested for their thermal response latency according to the timeline in (A). (B) IENF and SNP were analyzed in hind paw footskin in the three groups of animals. (C) DRG tissues from control, diabetic and IGF-1-treated diabetic rats were isolated and subjected to Complex I and Complex IV enzymatic activity assays. Data are in mU/mg tissue. In (A, B and C) data are mean ± SEM of N = 5–10; * = $p < 0.05$ or ** = $p < 0.01$ or *** = $p < 0.001$ or **** = $p < 0.0001$; analyzed by one-way ANOVA or two-way ANOVA with Tukey's *post-hoc* test.

cultures and adds a novel index of the therapeutic potential of IGF-1 against a structural manifestation of DSPN using an assay that reflects the human condition.

The mechanisms through which IGF-1 operates to implement nerve growth and repair are not completely understood. It has been proposed that optimal mitochondrial function is a key factor for axonal outgrowth and repair [50,51]. For instance, modulating mitochondrial dynamics by overexpression of MFN-2 or inhibition of DRP-1 regulated the direction and rate of neurite outgrowth in cultured retinal ganglion cells from rat embryos [52]. Mitochondrial biogenesis triggered by the AMPK-PGC-1α-Nrf1 pathway and energy supplementation was required for axonal outgrowth in rat cortical neurons [53]. Resveratrol, an activator of AMPK, drives axonal outgrowth and was protective against diabetic neuropathy in STZ-induced diabetic rats [44,54]. Growth factors IL-1β, IL-17A, ciliary neurotrophic factor, and insulin enhanced mitochondrial function and promoted neurite outgrowth, which correlated with protection from development of DSPN in animal models of type 1 diabetes [39,55–57]. Studies with modulators of heat shock protein function revealed that improved mitochondrial function was associated with prevention and reversal of diabetic neuropathy in type 1 and type 2 models of diabetes [58,59]. In the present work in cultured DRG neurons, we demonstrate the novel finding that a physiologically relevant concentration of IGF-1, which does not stimulate the insulin receptor [46], up-regulated mitochondrial respiration together with a dose-dependent stimulation of ATP production.

Recent studies also report IGF-1-mediated optimization of mitochondrial phenotype in other cell types and diseases. IGF-1 therapy corrected mitochondrial ATPase activity and inhibited caspase 3 and 9 activation in liver cells from aging rats [60]. Glutamine knock-in in striatal cells from the mutant Huntingtin (mHtt) mouse displayed a reduction in ROS production and caspase 3 activity and an elevation in Tfam and mitochondrial-encoded cytochrome c oxidase II proteins when treated with IGF-1 [35]. In cancer cell lines, exogenous IGF-1 sustains cell viability by stimulating mitochondrial biogenesis and BNIP3-induced mitophagy [61]. In the current study, in cultured DRG neurons derived from control or diabetic rats, IGF-1 exerted a novel up-regulatory effect on mitochondrial respiration, with a significant

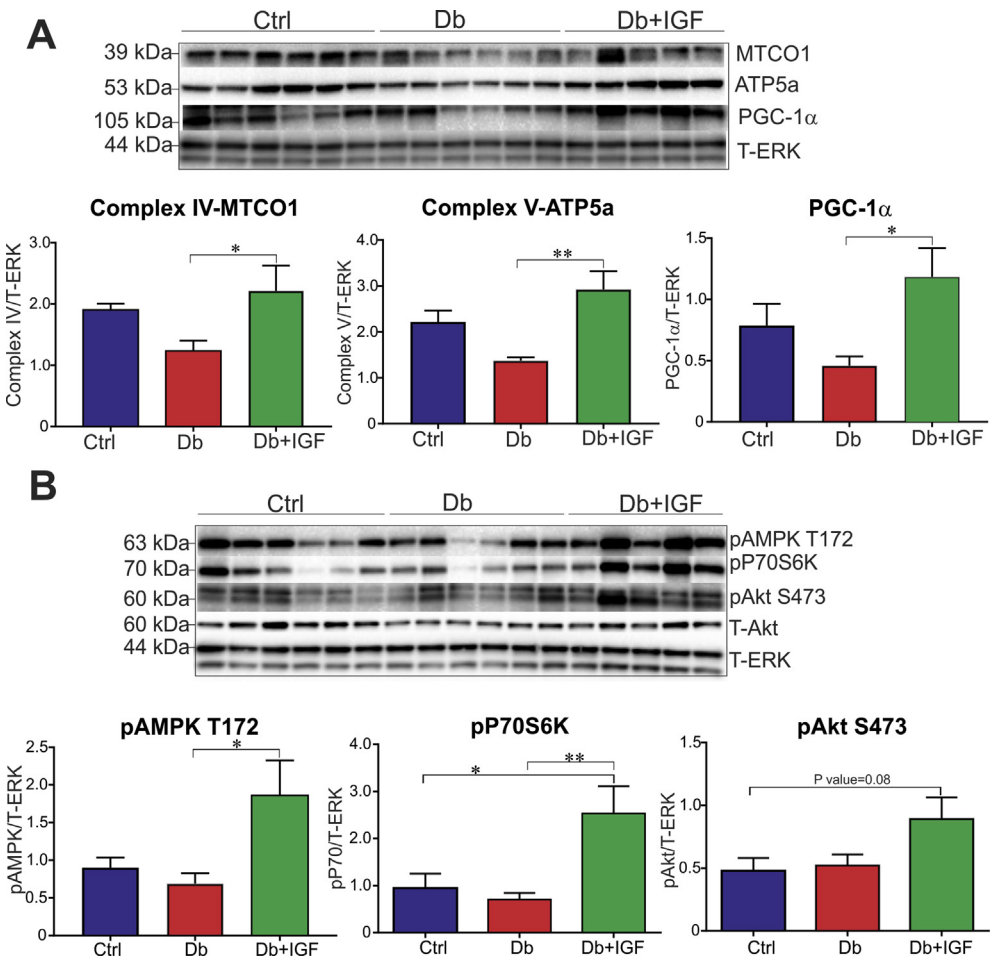

Figure 7: IGF-1 therapy restored the expression of PGC-1α and ETS proteins and up-regulated AMPK, P70S6K, and Akt phosphorylation in diabetic rats. DRG tissues from control (Ctrl), diabetic (Db) and IGF-1-treated diabetic (Db + IGF-1) rats were isolated and subjected to (A, B) Western blotting. Western blot band intensity of target proteins was normalized to total ERK bands of the same blot. Data are mean ± SEM of N = 5–7 animals; * = $p < 0.05$ or ** = $p < 0.01$; analyzed by one-way ANOVA with Tukey's *post-hoc* test.

stimulatory effect on spare, or reserve, respiratory capacity. This effect occurred over 24 h in control cultures and in diabetic cultures was triggered within 2 h. This may suggest that IGF-1 enhances the electrochemical gradient, as observed previously with insulin in DRG cultures [62], and aerobic glucose metabolism to elevate mitochondrial oxygen consumption rate [63–65]. In contrast to mitochondrial basal respiration, spare respiratory capacity is normally utilized when cells have excessive ATP demands or are stressed, as under chronic hyperglycemia. It is most likely that defects in expression or activity of respiratory chain complexes (or supercomplex formation) in diabetic conditions, essentially nutrient stress, drives suppression of spare respiratory capacity thus inducing an energy deficit [38,66,67]. IGF-1 may raise spare respiratory capacity through high ATP demand due to accelerated neurite outgrowth (thus optimizing the electrochemical gradient), and/or by normalizing aerobic glucose metabolism and/or via AMPK-dependent modulation of gene expression of ETS components.

Comparative mRNA quantitation of selective genes revealed that IGF-1, AMPK, and Akt isoforms, ATP5a1, MFN-1, and RHOT-1 were suppressed in DRG in diabetic rats. IGF-1 treatment of cultured DRGs from both control and diabetic rats improved the expression of these dysregulated genes with a higher impact in DRG neurons derived from diabetic rats. The most prominent finding of our gene expression analysis was that IGF-1 up-regulated AMPK (α1 and α2) and Akt (Akt1, Akt2, and Akt3) functional isoforms in cultured DRGs derived from diabetic rats. The transcriptional upregulation of these genes by IGF-1 in 6 h could be the main driving factor for enhanced mitochondrial respiration after 24 h IGF-1 treatment in cultured DRGs from both control and diabetic rats. Nevertheless, this does not seem to be the case for enhanced mitochondrial respiration after 2 h IGF-1 treatment, which is observed in diabetic cultures implying the involvement of post-translational modifications of metabolism-regulating proteins including AMPK and Akt.

AMPK and Akt pathways are modulated by IGF-1 in other cell types. In vascular smooth muscle cells, IGF-1 activates Akt to suppress AMPK activity by stimulating AMPK S485 phosphorylation, thus instigating AMPK T172 dephosphorylation [29]. There are two common upstream kinases, LKB-1 and CaMKKβ, known to phosphorylate AMPK on its activation site, T172, and activate this enzyme [68,69]. Our preliminary data (not shown) reveal that LKB-1 was not activated by IGF-1, and CaMKKβ inhibition by STO-609 did not significantly affect AMPK phosphorylation/activity (data not shown) or mitochondrial function in the presence of IGF-1 (Fig. 4B). In addition, we have preliminary data showing that IGF-1 did not induce a rise in intracellular Ca^{2+} in

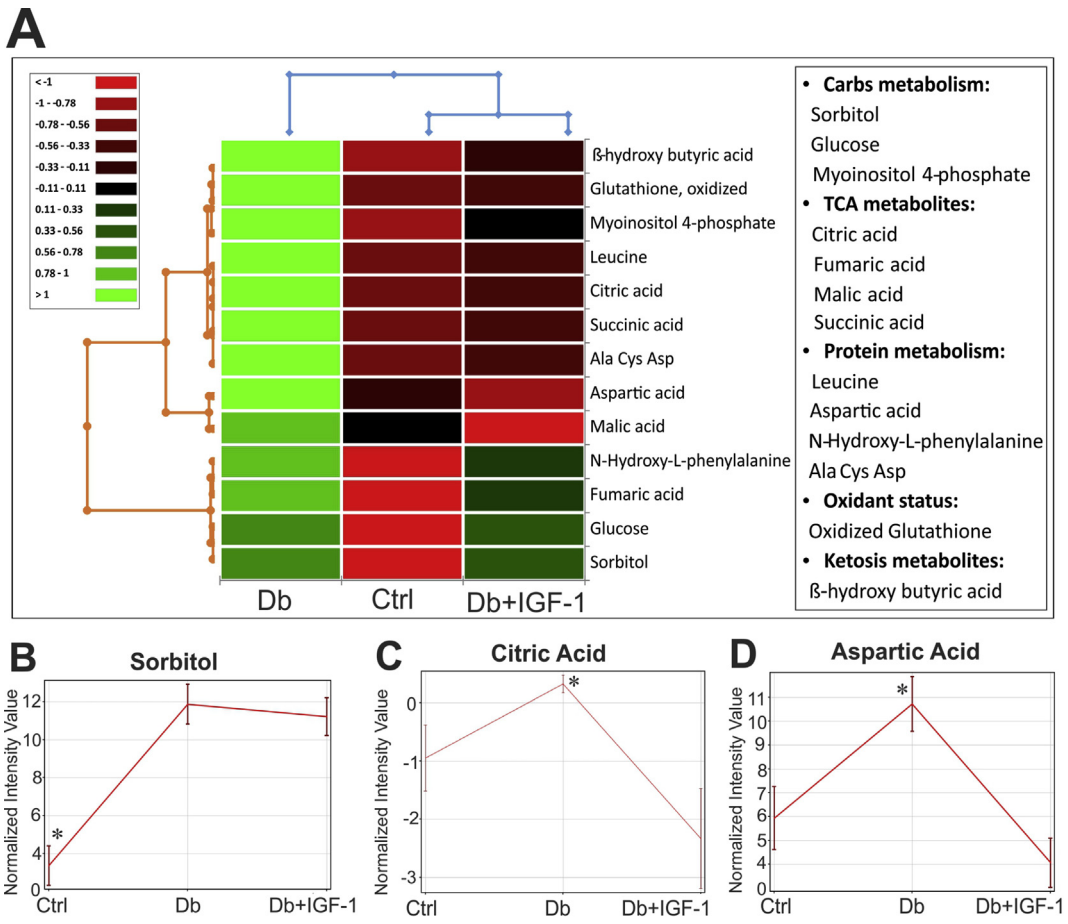

Figure 8: IGF-1 therapy reinstates the Krebs cycle, amino acid metabolism, ketosis and oxidant status in tibial nerve of diabetic rats. Tibial nerve tissues from control (Ctrl), diabetic (Db) and IGF-1-treated diabetic (Db + IGF-1) rats were dissected and weighed. Total metabolites were extracted using a methanol-water mixture, dried and subjected to metabolomic analysis using an HPLC system coupled to time-of-flight liquid chromatography/mass spectrometry. Normalized intensity value of each compound was estimated by using internal standards (L-Tryptophan-d5, L-Valine-d8, L-Alanine-d4, L-Leucine-d10, Citric Acid-d4, and D-Fructose). The final value for each metabolite was normalized to its corresponding tibial nerve weight and illustrated in (A) HeatMap. The trends for (B) sorbitol, (C) citric acid and (D) aspartic acid are shown as examples. Data are mean ± SEM of N = 9–12 animals; * = $p < 0.05$; analyzed by one-way ANOVA, followed by Benjamini-Hochberg multiple testing corrections.

cultured DRG neurons (where a rise in Ca^{2+} could be surmised to trigger activation of CaMKKβ). AMPK is also reported to be phosphorylated on T172 and activated in an ATM-dependent manner by IGF-1 in HeLa, PANC-1 and TIG103 cell lines [28] and so future studies will focus on this pathway.

Among different pharmacological inhibitors used to block IGF-1 downstream effectors, the AMPK inhibitor Compound C completely abolished the IGF-1-mediated up-regulation of mitochondrial maximal respiration and spare respiratory capacity. Neurite outgrowth was also blocked (Fig. 6). SiRNA-based inhibition of the AMPKα1 isoform, but not AMPKα2 isoform, exhibited a similar suppression of the IGF-1 enhancement of mitochondrial respiration and neurite outgrowth. The IGF-1 stimulation of mitochondrial DNA copy number was blocked by either AMPKα2 or AMPKα1 knockdown, which implicates both isoforms in mtDNA replication. A variety of functions have been reported for these two AMPK isoforms in other tissues. In striatal cells in mice with Huntington's disease (HD), accumulated Huntingtin resulted in AMPKα1 over-activation and nuclear translocation causing cell death through down-regulation of Bcl-2 [70]. AMPKα1 promotes contractile function of cardiomyocytes by phosphorylating troponin I [71], and myogenesis through myogenin gene expression [72]. AMPKα2 knock-out mice show deficient Complex I activity and lower cardiolipin content correlating with decreased cardiolipin synthetic enzymes in cardiomyocytes [73]. In endothelial cells, AMPKα2 activates anti-inflammatory pathways by phosphorylating PARP-1 and induction of Bcl-6 [74].

Acute (30 min) intrathecal application of IGF-1 activated Akt in DRG and this effect was diminished in *ob/ob* type 2 diabetic mice [75]. In our *in vitro* studies the Akt inhibitor, MK-2206, suppressed the IGF-1 dependent augmentation of mitochondrial function and neurite outgrowth (Figure 4B and 6). Previous work in smooth muscle cells and cancer cell lines revealed an inhibitory effect of Akt on AMPK via phosphorylation on S485/S487 and subsequent suppression of phosphorylation on T172 [29,76]. Moreover, we also found that inhibiting Akt results in higher AMPK T172 phosphorylation in cultured DRGs (data not shown). However, we have observed that the Akt inhibitor suppressed the IGF-1 up-regulation of mtDNA copy number (data not shown). In the present study, IGF-1 enhanced phosphorylation of P70S6K (Supplementary Figure 3D) and Akt directly elevates P70S6K activity and eukaryotic translation initiation factor 4E (eIF4E)-binding protein 1 (4E-BP1) function to augment ETS gene expression [77]. Thus, these studies utilizing pharmacological blockade of Akt reveal (i) in DRG neurons treated with IGF-1 Akt is acting upstream from AMPK to suppress AMPK activity, and (ii) upon IGF-1 treatment,

Akt is mediating parallel or alternative pathways from AMPK that regulate mitochondrial function and neurite outgrowth.

Previous studies reveal a role of impaired IGF-1 signaling in the etiology of diabetic neuropathy, or as a protective factor [6,7,24]. Mice with overexpression of neuron-specific IGF binding protein 5 (IGFBP5: an inhibitory IGF binding protein) or with depleted IGF1R expression displayed a progressive neurodegeneration similar to that seen in diabetic neuropathy. These deficits included motor axonopathy and sensory disorders such as thermal hypoalgesia and intra-epidermal nerve fiber loss [24]. Osmotic minipump implants releasing 4.2–4.8 μg/day IGF-1 or IGF-2 for two weeks prevented hyperalgesia and promoted nerve regeneration in STZ-diabetic rats that had a sciatic nerve crush injury [17,19]. In a similar study, STZ-induced diabetic rats exhibited loss of IENF after three months of diabetes, which was prevented by one-month intrathecal delivery of IGF-1 [20]. Five micromolar (5 μM) intrathecal infusion of IGF-1 for one month also improved sensory and motor nerve conduction velocities in diabetic rats [21].

We previously reported a significant loss of nerves of paw skin and concurrent hypoalgesia in 5 month diabetic rats and that insulin implants for the last four months prevented IENF loss and thermal hypoalgesia without correcting hyperglycemia [39]. In the present study, maintaining diabetic rats for 5 months did not cause significant nerve fiber loss in the foot skin compared to age-matched control rats, despite concurrent thermal hypoalgesia. There is precedence for this disassociation as thermal hypoalgesia precedes detectable IENF loss in STZ-diabetic mice [78]. It is notable that while our STZ-injected rats were clearly hyperglycemic, they were not in a state of extreme catabolic dominance as they gained weight over the study period and appear to model a slowly progressing neuropathy reflective of the human condition. The amelioration of thermal hypoalgesia by IGF-1 in diabetic rats could be due to enhanced sensitivity of afferents via such known properties as stimulation of T-type channels [79] or sensitization and translocation of the vanilloid receptor [80]. Alternately, as IGF-1 enhances substance P and CGRP expression in DRG cultures [81], it may protect against the diabetes-induced depletion of sensory neuron neuropeptide expression [82] and stimulus-evoked spinal release [83] that is associated with early stages of thermal hypoalgesia [78].

Nutrient flux analysis in *db/db* type 2 diabetic mice at 24 weeks of age showed an increase in flux of TCA intermediates in kidney but a decrease in sciatic nerve [84]. Metabolomic analysis of tibial nerves in the current study exhibited an increase in TCA intermediates in diabetic rats. Thus, if reduced flux of metabolites is occurring [84], this build-up of TCA intermediates suggests that a deficiency in ETS electron flow and/or enzyme activities is causing impaired utilization of the excessive available energy sources provided by the Krebs cycle under diabetic conditions. The diabetes-induced suppression of spare respiratory capacity combined with reduced ETS protein expression and activity of Complexes I and IV support the last statement. Despite no effect on up-regulated intracellular sorbitol and glucose in nerve in diabetes, IGF-1 therapy reinstated ketosis, lowered TCA intermediate build-up, and normalized oxidant status. Moreover, increased free amino acids or fragmented peptides in tibial nerves of diabetic rats demonstrate disturbed protein synthesis and metabolism, which were restored by IGF-1 therapy, correlating with higher phosphorylation of P70S6K in DRGs.

Given the established role of IGF-1 in neurite outgrowth, differentiation, and development, a plethora of nervous system-related diseases including Parkinson's disease, Alzheimer's disease, multiple sclerosis, amyotrophic lateral sclerosis, Fragile X syndrome, and Rett syndrome have become candidates for IGF-1 therapy [85]. A double-blind clinical trial of IGF-1 therapy in ALS patients receiving IGF-1 (0.5–3 μg/kg every two weeks for 40 weeks) resulted in beneficial effects with no adverse events [86]. A phase 1 clinical trial of IGF-1 therapy (40–120 μg/kg twice daily for 4 weeks) in 12 girls with Rett syndrome improved measures of anxiety, mood, and apnea with no serious adverse effects [87]. IGF-1 therapy remains a potential therapeutic option in diabetic neuropathy but has been hindered by other potential systemic actions of the peptide. Our studies reveal a novel aspect of IGF-1 signaling to augment the AMPK pathway to drive nerve repair. Specific targeting of the IGF-1 signaling axis in neurons could offer an alternative or complementary approach to treating neurological disease.

FUNDING

This work was supported by grant # MOP-130282 from the Canadian Institutes of Health Research to P.F. and grants NS081082 and 3DP3DK108245/T729934 from the National Institutes of Health to N.A.C. We are grateful to St Boniface Hospital Research for support.

AUTHOR CONTRIBUTIONS

M.R.A. designed and performed the *in vitro* studies and analyzed all tissues from the *in vivo* study. He aided in the metabolomic analysis and thermal sensitivity testing, performed data generation and analysis, and contributed to writing of the manuscript. D.S. directed maintenance of diabetic rats, performed thermal sensitivity testing, performed IGF-I therapy, and aided in data analysis and statistics. A.A. performed *in vitro* studies identifying IGF-1 as a regulator of AMPK. M.A., and S.S. performed metabolomic analysis and bioinformatics. C.A.J. and F.D. maintained and treated diabetic mice and performed imaging studies on the cornea. A.N. performed terminal analysis of corneal confocal measurements. X.Z. performed IENF analysis. N.A.C. supervised skin histopathology and corneal confocal microscopy studies and aided in writing of manuscript. P.F. supervised all *in vitro* and the *in vivo* rat work and wrote the manuscript.

ACKNOWLEDGMENTS

We would like to thank Dr. Mohammad Golam Sabbir, St Boniface Research Centre, for his contribution to 2D gel set up and Alex Marquez and Katie Frizzi for excellent technical support.

CONFLICT OF INTEREST

None.

APPENDIX A. SUPPLEMENTARY DATA

Supplementary data to this article can be found online at https://doi.org/10.1016/j.molmet.2018.11.008.

REFERENCES

[1] Vinik, A.I., Casellini, C., Névoret, M.L., 2016. Alternative quantitative tools in the assessment of diabetic peripheral and autonomic neuropathy. In: Calcutt, N.A., Fernyhough, P. (Eds.), International review of neurobiology, vol. 127. London: Academic Press. p. 235–85. https://doi.org/10.1016/bs.irn.2016.03.010.

[2] Zhuang, H.X., Wuarin, L., Fei, Z.J., Ishii, D.N., 1997. Insulin-like growth factor (IGF) gene expression is reduced in neural tissues and liver from rats with non-insulin-dependent diabetes mellitus, and IGF treatment ameliorates diabetic neuropathy. Journal of Pharmacology and Experimental Therapeutics 283(1): 366–374.

[3] Palta, M., LeCaire, T.J., Sadek-Badawi, M., Herrera, V.M., Danielson, K.K., 2014. The trajectory of IGF-1 across age and duration of type 1 diabetes. Diabetes Metabolism of Research Review 30(8):777–783. https://doi.org/10.1002/dmrr.2554.

[4] Ishii, D.N., Guertin, D.M., Whalen, L.R., 1994. Reduced insulin-like growth factor-I mRNA content in liver, adrenal glands and spinal cord of diabetic rats. Diabetologia 37(11):1073–1081.

[5] Ekstrom, A.R., Kanje, M., Skottner, A., 1989. Nerve regeneration and serum levels of insulin-like growth factor-I in rats with streptozotocin-induced insulin deficiency. Brain Research 496(1–2):141–147.

[6] Ishii, D.N., 1995. Implication of insulin-like growth factors in the pathogenesis of diabetic neuropathy. Brain Research in Brain Research Review 20(1):47–67.

[7] Rauskolb, S., Dombert, B., Sendtner, M., 2017. Insulin-like growth factor 1 in diabetic neuropathy and amyotrophic lateral sclerosis. Neurobiology of Disease 97(Pt B):103–113. https://doi.org/10.1016/j.nbd.2016.04.007.

[8] Zochodne, D.W., 2016. Sensory neurodegeneration in diabetes: beyond glucotoxicity. International Review of Neurobiology 127:151–180. https://doi.org/10.1016/bs.irn.2016.03.007.

[9] Zackenfels, K., Oppenheim, R.W., Rohrer, H., 1995. Evidence for an important role of IGF-I and IGF-II for the early development of chick sympathetic neurons. Neuron 14(4):731–741.

[10] Fernyhough, P., Willars, G.B., Lindsay, R.M., Tomlinson, D.R., 1993. Insulin and insulin-like growth factor I enhance regeneration in cultured adult rat sensory neurones. Brain Research 607(1–2):117–124.

[11] Recio-Pinto, E., Rechler, M.M., Ishii, D.N., 1986. Effects of insulin, insulin-like growth factor-II, and nerve growth factor on neurite formation and survival in cultured sympathetic and sensory neurons. Journal of Neuroscience 6(5): 1211–1219.

[12] Caroni, P., Schneider, C., Kiefer, M.C., Zapf, J., 1994. Role of muscle insulin-like growth factors in nerve sprouting: suppression of terminal sprouting in paralyzed muscle by IGF-binding protein 4. The Journal of Cell Biology 125(4): 893–902.

[13] Syroid, D.E., Zorick, T.S., Arbet-Engels, C., Kilpatrick, T.J., Eckhart, W., Lemke, G., 1999. A role for insulin-like growth factor-I in the regulation of Schwann cell survival. Journal of Neuroscience 19(6):2059–2068.

[14] Chattopadhyay, S., Shubayev, V.I., 2009. MMP-9 controls Schwann cell proliferation and phenotypic remodeling via IGF-1 and ErbB receptor-mediated activation of MEK/ERK pathway. Glia 57(12):1316–1325. https://doi.org/10.1002/glia.20851.

[15] Russell, J.W., Cheng, H.L., Golovoy, D., 2000. Insulin-like growth factor-I promotes myelination of peripheral sensory axons. Journal of Neuropathology and Experimental Neurology 59(7):575–584.

[16] Cheng, H.L., Steinway, M.L., Russell, J.W., Feldman, E.L., 2000. GTPases and phosphatidylinositol 3-kinase are critical for insulin-like growth factor-I-mediated Schwann cell motility. Journal of Biological Chemistry 275(35): 27197–27204. https://doi.org/10.1074/jbc.M002534200.

[17] Ishii, D.N., Lupien, S.B., 1995. Insulin-like growth factors protect against diabetic neuropathy: effects on sensory nerve regeneration in rats. Journal of Neuroscience Research 40(1):138–144. https://doi.org/10.1002/jnr.490400116.

[18] Sjoberg, J., Kanje, M., 1989. Insulin-like growth factor (IGF-1) as a stimulator of regeneration in the freeze-injured rat sciatic nerve. Brain Research 485(1): 102–108.

[19] Zhuang, H.X., Snyder, C.K., Pu, S.F., Ishii, D.N., 1996. Insulin-like growth factors reverse or arrest diabetic neuropathy: effects on hyperalgesia and impaired nerve regeneration in rats. Experimental Neurology 140(2):198–205. https://doi.org/10.1006/exnr.1996.0129.

[20] Toth, C., Brussee, V., Zochodne, D.W., 2006. Remote neurotrophic support of epidermal nerve fibres in experimental diabetes. Diabetologia 49(5): 1081–1088. https://doi.org/10.1007/s00125-006-0169-8.

[21] Brussee, V., Cunningham, F.A., Zochodne, D.W., 2004. Direct insulin signaling of neurons reverses diabetic neuropathy. Diabetes 53(7):1824–1830.

[22] Homs, J., Pages, G., Ariza, L., Casas, C., Chillon, M., Navarro, X., et al., 2014. Intrathecal administration of IGF-I by AAVrh10 improves sensory and motor deficits in a mouse model of diabetic neuropathy. Molecular Therapeutics Methods in Clinical Development 1:7. https://doi.org/10.1038/mtm.2013.7.

[23] Chu, Q., Moreland, R., Yew, N.S., Foley, J., Ziegler, R., Scheule, R.K., 2008. Systemic Insulin-like growth factor-1 reverses hypoalgesia and improves mobility in a mouse model of diabetic peripheral neuropathy. Molecular Therapy 16(8):1400–1408. https://doi.org/10.1038/mt.2008.115.

[24] Simon, C.M., Rauskolb, S., Gunnersen, J.M., Holtmann, B., Drepper, C., Dombert, B., et al., 2015. Dysregulated IGFBP5 expression causes axon degeneration and motoneuron loss in diabetic neuropathy. Acta Neuropathologica 130(3):373–387. https://doi.org/10.1007/s00401-015-1446-8.

[25] Le Roith, D., Zick, Y., 2001. Recent advances in our understanding of insulin action and insulin resistance. Diabetes Care 24(3):588–597.

[26] Cheng, Z., Tseng, Y., White, M.F., 2010. Insulin signaling meets mitochondria in metabolism. Trends in Endocrinology and Metabolism 21(10):589–598. https://doi.org/10.1016/j.tem.2010.06.005.

[27] Xi, G., Rosen, C.J., Clemmons, D.R., 2016. IGF-I and IGFBP-2 stimulate AMPK activation and autophagy, which are required for osteoblast differentiation. Endocrinology 157(1):268–281. https://doi.org/10.1210/en.2015-1690.

[28] Suzuki, A., Kusakai, G., Kishimoto, A., Shimojo, Y., Ogura, T., Lavin, M.F., et al., 2004. IGF-1 phosphorylates AMPK-alpha subunit in ATM-dependent and LKB1-independent manner. Biochemical and Biophysical Research Communications 324(3):986–992. https://doi.org/10.1016/j.bbrc.2004.09.145.

[29] Ning, J., Xi, G., Clemmons, D.R., 2011. Suppression of AMPK activation via S485 phosphorylation by IGF-I during hyperglycemia is mediated by AKT activation in vascular smooth muscle cells. Endocrinology 152(8):3143–3154. https://doi.org/10.1210/en.2011-0155.

[30] Canto, C., Auwerx, J., 2009. PGC-1alpha, SIRT1 and AMPK, an energy sensing network that controls energy expenditure. Current Opinion in Lipidology 20(2): 98–105. https://doi.org/10.1097/MOL.0b013e328328d0a4.

[31] Green, M.F., Scott, J.W., Steel, R., Oakhill, J.S., Kemp, B.E., Means, A.R., 2011. Ca2+/Calmodulin-dependent protein kinase kinase beta is regulated by multisite phosphorylation. Journal of Biological Chemistry 286(32): 28066–28079. https://doi.org/10.1074/jbc.M111.251504.

[32] Logan, S., Pharaoh, G.A., Marlin, M.C., Masser, D.R., Matsuzaki, S., Wronowski, B., et al., 2018. Insulin-like growth factor receptor signaling regulates working memory, mitochondrial metabolism, and amyloid-beta uptake in astrocytes. Molecular Metabolism 9:141–155. https://doi.org/10.1016/j.molmet.2018.01.013.

[33] Naia, L., Ribeiro, M., Rodrigues, J., Duarte, A.I., Lopes, C., Rosenstock, T.R., et al., 2016. Insulin and IGF-1 regularize energy metabolites in neural cells expressing full-length mutant huntingtin. Neuropeptides 58:73–81. https://doi.org/10.1016/j.npep.2016.01.009.

[34] Gazit, N., Vertkin, I., Shapira, I., Helm, M., Slomowitz, E., Sheiba, M., et al., 2016. IGF-1 receptor differentially regulates spontaneous and evoked transmission via mitochondria at hippocampal synapses. Neuron 89(3):583–597. https://doi.org/10.1016/j.neuron.2015.12.034.

[35] Ribeiro, M., Rosenstock, T.R., Oliveira, A.M., Oliveira, C.R., Rego, A.C., 2014. Insulin and IGF-1 improve mitochondrial function in a PI-3K/Akt-dependent manner and reduce mitochondrial generation of reactive oxygen species in Huntington's disease knock-in striatal cells. Free Radical Biology and Medicine 74:129–144. https://doi.org/10.1016/j.freeradbiomed.2014.06.023.

[36] Mootha, V.K., Lindgren, C.M., Eriksson, K.F., Subramanian, A., Sihag, S., Lehar, J., et al., 2003. PGC-1alpha-responsive genes involved in oxidative phosphorylation are coordinately downregulated in human diabetes. Nature Genetics 34(3):267–273. https://doi.org/10.1038/ng1180.

[37] Patti, M.E., Butte, A.J., Crunkhorn, S., Cusi, K., Berria, R., Kashyap, S., et al., 2003. Coordinated reduction of genes of oxidative metabolism in humans with insulin resistance and diabetes: potential role of PGC1 and NRF1. Proceedings of the National Academy of Sciences of the United States of America 100(14): 8466–8471. https://doi.org/10.1073/pnas.1032913100.

[38] Fernyhough, P., 2015. Mitochondrial dysfunction in diabetic neuropathy: a series of unfortunate metabolic events. Current Diabetes Reports 15(11):89. https://doi.org/10.1007/s11892-015-0671-9.

[39] Aghanoori, M.R., Smith, D.R., Roy Chowdhury, S., Sabbir, M.G., Calcutt, N.A., Fernyhough, P., 2017. Insulin prevents aberrant mitochondrial phenotype in sensory neurons of type 1 diabetic rats. Experimental Neurology 297:148–157. https://doi.org/10.1016/j.expneurol.2017.08.005.

[40] Lupien, S.B., Bluhm, E.J., Ishii, D.N., 2003. Systemic insulin-like growth factor-I administration prevents cognitive impairment in diabetic rats, and brain IGF regulates learning/memory in normal adult rats. Journal of Neuroscience Research 74(4):512–523. https://doi.org/10.1002/jnr.10791.

[41] Jolivalt, C.G., Frizzi, K.E., Guernsey, L., Marquez, A., Ochoa, J., Rodriguez, M., et al., 2016. Peripheral neuropathy in mouse models of diabetes. Current Protocol in Mouse Biology 6(3):223–255. https://doi.org/10.1002/cpmo.11.

[42] Chen, D.K., Frizzi, K.E., Guernsey, L.S., Ladt, K., Mizisin, A.P., Calcutt, N.A., 2013. Repeated monitoring of corneal nerves by confocal microscopy as an index of peripheral neuropathy in type-1 diabetic rodents and the effects of topical insulin. Journal of the Peripheral Nervous System 18(4):306–315. https://doi.org/10.1111/jns5.12044.

[43] Calcutt, N.A., Smith, D.R., Frizzi, K., Sabbir, M.G., Chowdhury, S.K., Mixcoatl-Zecuatl, T., et al., 2017. Selective antagonism of muscarinic receptors is neuroprotective in peripheral neuropathy. Journal of Clinical Investigation 127(2):608–622. https://doi.org/10.1172/JCI88321.

[44] Roy Chowdhury, S.K., Smith, D.R., Saleh, A., Schapansky, J., Marquez, A., Gomes, S., et al., 2012. Impaired adenosine monophosphate-activated protein kinase signalling in dorsal root ganglia neurons is linked to mitochondrial dysfunction and peripheral neuropathy in diabetes. Brain 135(Pt 6): 1751–1766. https://doi.org/10.1093/brain/aws097.

[45] Hanson, M., Zahradka, P., Taylor, C.G., Aliani, M., 2018. Identification of urinary metabolites with potential blood pressure-lowering effects in lentil-fed spontaneously hypertensive rats. European Journal of Nutrition 57(1): 297–308. https://doi.org/10.1007/s00394-016-1319-5.

[46] Recio-Pinto, E., Ishii, D.N., 1988. Insulin and insulinlike growth factor receptors regulating neurite formation in cultured human neuroblastoma cells. Journal of Neuroscience Research 19(3):312–320. https://doi.org/10.1002/jnr.490190306.

[47] Freeman, O.J., Unwin, R.D., Dowsey, A.W., Begley, P., Ali, S., Hollywood, K.A., et al., 2016. Metabolic dysfunction is restricted to the sciatic nerve in experimental diabetic neuropathy. Diabetes 65(1):228–238. https://doi.org/10.2337/db15-0835.

[48] Tavakoli, M., Petropoulos, I.N., Malik, R.A., 2013. Corneal confocal microscopy to assess diabetic neuropathy: an eye on the foot. Journal of Diabetes Science Technology 7(5):1179–1189. https://doi.org/10.1177/193229681300700509.

[49] Davidson, E.P., Coppey, L.J., Yorek, M.A., 2012. Early loss of innervation of cornea epithelium in streptozotocin-induced type 1 diabetic rats: improvement with ilepatril treatment. Investigative Ophthalmology and Visual Science 53(13):8067–8074. https://doi.org/10.1167/iovs.12-10826.

[50] Chowdhury, S.K., Smith, D.R., Fernyhough, P., 2013. The role of aberrant mitochondrial bioenergetics in diabetic neuropathy. Neurobiology of Disease 51:56–65. https://doi.org/10.1016/j.nbd.2012.03.016.

[51] Cashman, C.R., Hoke, A., 2015. Mechanisms of distal axonal degeneration in peripheral neuropathies. Neuroscience Letters 596:33–50. https://doi.org/10.1016/j.neulet.2015.01.048.

[52] Steketee, M.B., Moysidis, S.N., Weinstein, J.E., Kreymerman, A., Silva, J.P., Iqbal, S., et al., 2012. Mitochondrial dynamics regulate growth cone motility, guidance, and neurite growth rate in perinatal retinal ganglion cells in vitro. Investigative Ophthalmology and Visual Science 53(11):7402–7411. https://doi.org/10.1167/iovs.12-10298.

[53] Vaarmann, A., Mandel, M., Zeb, A., Wareski, P., Liiv, J., Kuum, M., et al., 2016. Mitochondrial biogenesis is required for axonal growth. Development 143(11):1981–1992. https://doi.org/10.1242/dev.128926.

[54] Dasgupta, B., Milbrandt, J., 2007. Resveratrol stimulates AMP kinase activity in neurons. Proceedings of the National Academy of Sciences of the United States of America 104(17):7217–7222. https://doi.org/10.1073/pnas.0610068104.

[55] Habash, T., Saleh, A., Roy Chowdhury, S.K., Smith, D.R., Fernyhough, P., 2015. The proinflammatory cytokine, interleukin-17A, augments mitochondrial function and neurite outgrowth of cultured adult sensory neurons derived from normal and diabetic rats. Experimental Neurology 273:177–189. https://doi.org/10.1016/j.expneurol.2015.08.016.

[56] Saleh, A., Chowdhury, S.K., Smith, D.R., Balakrishnan, S., Tessler, L., Schartner, E., et al., 2013. Diabetes impairs an interleukin-1beta-dependent pathway that enhances neurite outgrowth through JAK/STAT3 modulation of mitochondrial bioenergetics in adult sensory neurons. Molecular Brain 6:45. https://doi.org/10.1186/1756-6606-6-45.

[57] Saleh, A., Roy Chowdhury, S.K., Smith, D.R., Balakrishnan, S., Tessler, L., Martens, C., et al., 2013. Ciliary neurotrophic factor activates NF-kappaB to enhance mitochondrial bioenergetics and prevent neuropathy in sensory neurons of streptozotocin-induced diabetic rodents. Neuropharmacology 65: 65–73. https://doi.org/10.1016/j.neuropharm.2012.09.015.

[58] Ma, J., Farmer, K.L., Pan, P., Urban, M.J., Zhao, H., Blagg, B.S., et al., 2014. Heat shock protein 70 is necessary to improve mitochondrial bioenergetics and reverse diabetic sensory neuropathy following KU-32 therapy. Journal of Pharmacology and Experimental Therapeutics 348(2):281–292. https://doi.org/10.1124/jpet.113.210435.

[59] Urban, M.J., Li, C., Yu, C., Lu, Y., Krise, J.M., McIntosh, M.P., et al., 2010. Inhibiting heat-shock protein 90 reverses sensory hypoalgesia in diabetic mice. ASN Neurology 2(4):e00040. https://doi.org/10.1042/AN20100015.

[60] Puche, J.E., Garcia-Fernandez, M., Muntane, J., Rioja, J., Gonzalez-Baron, S., Castilla Cortazar, I., 2008. Low doses of insulin-like growth factor-I induce mitochondrial protection in aging rats. Endocrinology 149(5):2620–2627. https://doi.org/10.1210/en.2007-1563.

[61] Lyons, A., Coleman, M., Riis, S., Favre, C., O'Flanagan, C.H., Zhdanov, A.V., et al., 2017. Insulin-like growth factor 1 signaling is essential for mitochondrial biogenesis and mitophagy in cancer cells. Journal of Biological Chemistry 292(41):16983–16998. https://doi.org/10.1074/jbc.M117.792838.

[62] Huang, T.J., Price, S.A., Chilton, L., Calcutt, N.A., Tomlinson, D.R., Verkhratsky, A., et al., 2003. Insulin prevents depolarization of the mitochondrial inner membrane in sensory neurons of type 1 diabetic rats in the presence of sustained hyperglycemia. Diabetes 52(8):2129–2136.

[63] Poburko, D., Santo-Domingo, J., Demaurex, N., 2011. Dynamic regulation of the mitochondrial proton gradient during cytosolic calcium elevations. Journal of Biological Chemistry 286(13):11672–11684. https://doi.org/10.1074/jbc.M110.159962.

[64] Cardoso, A.R., Queliconi, B.B., Kowaltowski, A.J., 2010. Mitochondrial ion transport pathways: role in metabolic diseases. Biochimica et Biophysica Acta 1797(6–7):832–838. https://doi.org/10.1016/j.bbabio.2009.12.017.

[65] Okorodudu, A.O., Adegboyega, P.A., Scholz, C.I., 1995. Intracellular calcium and hydrogen ions in diabetes mellitus. Annals of Clinical Laboratory Science 25(5):394–401.

[66] Sansbury, B.E., Jones, S.P., Riggs, D.W., Darley-Usmar, V.M., Hill, B.G., 2011. Bioenergetic function in cardiovascular cells: the importance of the reserve capacity and its biological regulation. Chemico Biological Interactions 191(1–3):288–295. https://doi.org/10.1016/j.cbi.2010.12.002.

[67] Rossignol, R., Faustin, B., Rocher, C., Malgat, M., Mazat, J.P., Letellier, T., 2003. Mitochondrial threshold effects. Biochemical Journal 370(Pt 3):751–762. https://doi.org/10.1042/BJ20021594.

[68] Hawley, S.A., Pan, D.A., Mustard, K.J., Ross, L., Bain, J., Edelman, A.M., et al., 2005. Calmodulin-dependent protein kinase kinase-beta is an alternative upstream kinase for AMP-activated protein kinase. Cell Metabolism 2(1):9–19. https://doi.org/10.1016/j.cmet.2005.05.009.

[69] Shaw, R.J., Kosmatka, M., Bardeesy, N., Hurley, R.L., Witters, L.A., DePinho, R.A., et al., 2004. The tumor suppressor LKB1 kinase directly activates AMP-activated kinase and regulates apoptosis in response to energy stress. Proceedings of the National Academy of Sciences of the United States of America 101(10):3329–3335. https://doi.org/10.1073/pnas.0308061100.

[70] Ju, T.C., Chen, H.M., Lin, J.T., Chang, C.P., Chang, W.C., Kang, J.J., et al., 2011. Nuclear translocation of AMPK-alpha1 potentiates striatal neurodegeneration in Huntington's disease. The Journal of Cell Biology 194(2): 209–227. https://doi.org/10.1083/jcb.201105010.

[71] Chen, S., Zhu, P., Guo, H.M., Solis, R.S., Wang, Y., Ma, Y., et al., 2014. Alpha1 catalytic subunit of AMPK modulates contractile function of cardiomyocytes through phosphorylation of troponin I. Life Sciences 98(2):75–82. https://doi.org/10.1016/j.lfs.2014.01.006.

[72] Fu, X., Zhao, J.X., Zhu, M.J., Foretz, M., Viollet, B., Dodson, M.V., et al., 2013. AMP-activated protein kinase alpha1 but not alpha2 catalytic subunit potentiates myogenin expression and myogenesis. Molecular and Cellular Biology 33(22):4517–4525. https://doi.org/10.1128/MCB.01078-13.

[73] Athea, Y., Viollet, B., Mateo, P., Rousseau, D., Novotova, M., Garnier, A., et al., 2007. AMP-activated protein kinase alpha2 deficiency affects cardiac cardiolipin homeostasis and mitochondrial function. Diabetes 56(3):786–794. https://doi.org/10.2337/db06-0187.

[74] Gongol, B., Marin, T., Peng, I.C., Woo, B., Martin, M., King, S., et al., 2013. AMPKα2 exerts its anti-inflammatory effects through PARP-1 and Bcl-6. Proceedings of the National Academy of Sciences of the United States of America 110(8):3161–3166. https://doi.org/10.1073/pnas.1222051110.

[75] Grote, C.W., Groover, A.L., Ryals, J.M., Geiger, P.C., Feldman, E.L., Wright, D.E., 2013. Peripheral nervous system insulin resistance in ob/ob mice. Acta Neuropathology Communication 1:15. https://doi.org/10.1186/2051-5960-1-15.

[76] Hawley, S.A., Ross, F.A., Gowans, G.J., Tibarewal, P., Leslie, N.R., Hardie, D.G., 2014. Phosphorylation by Akt within the ST loop of AMPK-alpha1 down-regulates its activation in tumour cells. Biochemical Journal 459(2): 275–287. https://doi.org/10.1042/BJ20131344.

[77] Goo, C.K., Lim, H.Y., Ho, Q.S., Too, H.P., Clement, M.V., Wong, K.P., 2012. PTEN/Akt signaling controls mitochondrial respiratory capacity through 4E-BP1. PLoS One 7(9):e45806. https://doi.org/10.1371/journal.pone.0045806.

[78] Beiswenger, K.K., Calcutt, N.A., Mizisin, A.P., 2008. Dissociation of thermal hypoalgesia and epidermal denervation in streptozotocin-diabetic mice. Neuroscience Letters 442(3):267–272. https://doi.org/10.1016/j.neulet.2008.06.079.

[79] Zhang, Y., Qin, W., Qian, Z., Liu, X., Wang, H., Gong, S., et al., 2014. Peripheral pain is enhanced by insulin-like growth factor 1 through a G protein-mediated stimulation of T-type calcium channels. Science Signaling 7(346): ra94. https://doi.org/10.1126/scisignal.2005283.

[80] Van Buren, J.J., Bhat, S., Rotello, R., Pauza, M.E., Premkumar, L.S., 2005. Sensitization and translocation of TRPV1 by insulin and IGF-I. Molecular Pain 1: 17. https://doi.org/10.1186/1744-8069-1-17.

[81] Liu, Z., Liu, H., Yang, X., Xu, X., Zhang, W., Li, Z., 2010. Effects of insulin-like growth factor-1 on expression of sensory neuropeptides in cultured dorsal root ganglion neurons in the absence or presence of glutamate. International Journal of Neuroscience 120(11):698–702. https://doi.org/10.3109/00207454.2010.513463.

[82] Diemel, L.T., Brewster, W.J., Fernyhough, P., Tomlinson, D.R., 1994. Expression of neuropeptides in experimental diabetes; effects of treatment with nerve growth factor or brain-derived neurotrophic factor. Brain Research in Molecular Brain Research 21(1–2):171–175.

[83] Calcutt, N.A., Stiller, C., Gustafsson, H., Malmberg, A.B., 2000. Elevated substance-P-like immunoreactivity levels in spinal dialysates during the formalin test in normal and diabetic rats. Brain Research 856(1–2):20–27.

[84] Sas, K.M., Kayampilly, P., Byun, J., Nair, V., Hinder, L.M., Hur, J., et al., 2016. Tissue-specific metabolic reprogramming drives nutrient flux in diabetic complications. JCI Insight 1(15):e86976. https://doi.org/10.1172/jci.insight.86976.

[85] Costales, J., Kolevzon, A., 2016. The therapeutic potential of insulin-like growth factor-1 in central nervous system disorders. Neuroscience and Biobehavioral Reviews 63:207–222. https://doi.org/10.1016/j.neubiorev.2016.01.001.

[86] Nagano, I., Shiote, M., Murakami, T., Kamada, H., Hamakawa, Y., Matsubara, E., et al., 2005. Beneficial effects of intrathecal IGF-1 administration in patients with amyotrophic lateral sclerosis. Neurological Research 27(7):768–772. https://doi.org/10.1179/016164105X39860.

[87] Khwaja, O.S., Ho, E., Barnes, K.V., O'Leary, H.M., Pereira, L.M., Finkelstein, Y., et al., 2014. Safety, pharmacokinetics, and preliminary assessment of efficacy of mecasermin (recombinant human IGF-1) for the treatment of Rett syndrome. Proceedings of the National Academy of Sciences of the United States of America 111(12):4596–4601. https://doi.org/10.1073/pnas.1311141111.

